

CI/SIB 9	(K4f)	CP 30/73
-------------	-------	-------------

November 1973

Wind pressure and strain measurements at the Post Office Tower

C W Newberry, K J Eaton and J R Mayne

Building Research Station

Current papers

Current Papers are circulated to selected audience groups appropriate to each subject. Full details of all recent Current Papers and other BRE Publications are published quarterly in BRE NEWS. Requests for BRE NEWS or for placing on the Current Paper mailing list should be addressed to:

**Distribution Unit,
Application Services Division,
Building Research Establishment,
Garston, Watford.WD2 7JR.**

Extra copies of this paper are available; a charge may be made for supplies in quantity.



WIND PRESSURE AND STRAIN MEASUREMENTS AT THE POST OFFICE TOWER

C W Newberry, BSc(Eng), MIMechE, FRPS, K J Eaton, BSc(Eng), PhD, FRMetS and
J R Mayne, BSc

This paper presents some results not previously published of the full-scale wind loading project carried out at the Post Office Tower, London. Autocorrelations and pressure spectra were determined for all the pressure transducers, and the variations of these around the structure as well as vertically are discussed. The effect of vortex shedding from the Tower on the cladding loads is also shown. At each level where transducers were installed, the pressures were combined to give total horizontal loads and an important result from this is that, in general, the short duration loads were greatest at the lower heights due to high transient suctions in the lee of the structure. The significance of gust sizes is discussed and recommendations are made for design gust durations.

The dynamic movement of the Tower was measured by strain gauges near the base of the shaft. Large deflections transverse to the mean wind direction were recorded, the natural frequency being 0.157 Hz (ie 6.37 seconds/cycle). This agrees well with the estimated value when the structure was designed.

WIND PRESSURE AND STRAIN MEASUREMENTS AT THE POST OFFICE TOWER

by C W Newberry, K J Eaton and J R Mayne

INTRODUCTION

As part of the research programme undertaken by the Building Research Station to investigate wind loads and the effects of wind on tall buildings, measurements were made of wind pressures and the structural strain produced by them on the Post Office Tower in London. A description of the Tower and the instrumentation has been given in earlier papers^{1,2,3} together with some preliminary findings, but a more complete survey and analysis of the measurements has now been possible and is presented in this account of the investigation. For completeness, a brief summary of the description of the Tower and the instrumentation is repeated here.

The Tower (Figure 1) consists basically of a circular hollow shaft of reinforced concrete acting as a vertical cantilever. The shaft rises to a height of 177 m above ground level, and is generally about 7 m in diameter with an increase towards the base. Surrounding the shaft are a number of annular floors, most of which are enclosed by two cylindrical glass envelopes. The lower one extends from 35 m above ground to 110 m and is about 15.8 m in diameter, and the section is actually an 18-sided polygon rather than a true circle. Above this clad portion are a few unclad floors housing the aeriels. The upper cylindrical envelope, which is 48-sided, extends from 147 m to 170 m and varies in external diameter between about 15.5 m and 19.5 m.

Pressure transducers were installed at nine different levels in the cladding of the Tower at positions indicated in Figure 2. At four of these levels - B3, B7, B15 and D3, at heights of 49 m, 67 m, 104 m and 152 m respectively - there were complete rings of twelve transducers at 30° intervals around the Tower (with the exception of one channel on level D3) as indicated in Figure 3. At each of the other five levels - B5, B9, B11, B13 and D6 at 58 m, 76 m, 85 m, 94 m and 168 m respectively, three transducers were placed at 30° intervals in the south-west quadrant of the Tower to face the prevailing wind. They corresponded to positions 8, 9 and 10 in Figure 3. All the pressure transducers recorded the external cladding pressure on the Tower relative to a common reference pressure which closely approximated to that of the static head of the free atmosphere. Throughout this report channels are identified by their position around the Tower and the floor number, eg 10D3, 7B15, 1B3.

To record the dynamic response of the Tower to wind action, strain gauges were attached to the vertical reinforcement of the Tower shaft just above an anchoring link which tied the lower part of the Tower to an adjoining telephone exchange building. They were at level A8 as shown in Figure 2. At this level the shaft is an 11 m diameter reinforced concrete tube with 0.6 m thick walls. The reinforcement was arranged in two concentric rings near the inner and outer surfaces of the shaft, and the strain gauges were mounted on 12 bars of each ring at positions spaced at 30° intervals round the Tower.

The correlation of wind pressure and strain measurements with wind speed was achieved by recording the output of an anemometer mounted on a lattice mast on the top of the Tower at a height of 195 m. Additionally, for a limited period, two other anemometers mounted on a nearby mast at heights of 61 m and 43 m enabled simultaneous recording of wind speed at three heights to be made.

All the recordings of wind speed, wind pressure, and strain, with channels selected as required on any occasion, were made by means of multi-channel galvanometer recorders with synchronised charts running at speeds of 1 mm/second or 10 mm/second. From these charts, digitised data were read off at 1 second or 0.1 second intervals and transcribed to paper tape for computer analysis. The recordings analysed are listed in Table 1. It will be noticed that records 1 to 9 covered the vertical distribution of pressure up the windward side of the Tower, while records 10 to 20 were aimed at the study of the distribution of pressure around the Tower with two of them also recording the strain. A representative sample of an analogue record and the corresponding digital data is given in the Appendix.

The basic objectives of the analysis were to obtain data relating to cladding loads on the Tower at various heights and averaged over a range of load-averaging durations, to obtain data on the structural wind loads at various heights and for the Tower as a whole, also over a range of averaging periods, and to examine the response of the Tower to wind action. With such data available it was then expected that it would be possible to draw general conclusions relating wind loading parameters to structural and cladding design for tall buildings in a city environment.

COMPUTATION PROCEDURES

The methods used to carry out these calculations have been previously described in some detail^{3,4,5} but are briefly repeated here. With the large amount of data that were involved, the time-averaged pressures and loads were calculated and stored throughout the length of each record by processing 60 seconds of record at a time. Tables of maximum and minimum pressures and loads were then printed at the end of the calculation; these were inspected to locate the periods where extreme structural loads and cladding loads had occurred and then the results were output for these periods.

To compute total horizontal loads on one floor of the Tower, components were taken of each of the twelve pressure values at that level, and the resultant was determined. These resultant loads were computed for averaging times varying from 1 to 60 seconds, and the variation in loads could be observed second by second.

Methods described by Bendat and Piersol⁶ were used to compute autocorrelations and spectra for all the pressure transducers, and cross-correlations and coherence functions for various pairs of pressure transducers, particularly those vertically above one another on the windward side of the Tower. Since the data for any one record were split into parts - either a ring of twelve channels from one floor, or a vertical scan of nine channels - it was convenient to have this information in store in the computer in order to obtain these cross-correlations. The autocorrelation function describes the general dependence of the pressure values at one time on those at another time. The associated pressure spectrum represents the distribution of the variance of the pressure fluctuations according to frequency. The cross-correlation and coherence functions of the pressures recorded at pairs of transducers can be used to provide estimates of the size of gusts experienced by the Tower.

While strains were being measured at the base of the Tower, similar analyses were carried out on the strain gauge outputs. Mean and rms values were obtained and then autocorrelation functions and spectra were determined. It was also possible to resolve the strain values from the twelve points around the concrete shaft in order to study the movement of the Tower.

The records that were taken with three anemometers in position have been studied in detail in order to assess the variation in velocity with height. This work was mainly carried out by the Meteorological Office and is reported elsewhere^{4,7,8,9}.

RESULTS OF ANALYSIS

Cladding loads

The results of the variations of the surface pressure measurements (variations around the Tower and vertically up the structure) for the records listed in Table 1 have been published previously¹. Further work is continuing on this subject by analysing some other records that were taken at a faster recording speed; this will enable pressure fluctuations as short as 0.01 second to be investigated, and these results will be published in the near future.

Typical plots of the autocorrelation function for two vertical scans, during record 8, are shown in Figures 4 and 5. Vertical scan 10 (Figure 4) approximately faced the mean wind direction, and shows a general decrease in correlation with increasing time lag indicating that, for example, at a lag of 10 seconds the pressure on channel 10B11 was on average 0.5 of its value at any particular time. The best correlation is at level B11 (in the middle of the B-floors of the Tower), the next best is B15, then come D6 and B7 which are getting more turbulent and are therefore not correlated so well (D6 being near the top with various projections), and the floor showing the lowest correlation is B3, confirming that at this level the turbulence has increased considerably and therefore there is less likelihood of predicting the pressure that will occur at a lag of t seconds. The other four floors, B5, B9, B13 and D3, although for clarity not shown, fit in very well with the general progression in the correlations.

Figure 5 shows more results from the same record, but this time for vertical scan 8 which is 60° around the Tower and therefore very close to the separation point. Here the correlations for floors B11 and B15 are the highest; B7 is much lower, with some indication of 'humps' (ie some possible periodicity in the pressures or suction); the top of the Tower (D6) and the bottom (B3) are very poorly correlated, in just the same way as the windward side. Again, the other four floors fit in the general progression very well.

The next three figures show some typical results (record 16) for the variation in the auto-correlation around the Tower at three different levels. For ease of identifying the windward position etc, both mean and rms pressure coefficients (with respect to the velocity at the top of the Tower, \bar{V}_{195}) have also been included.

Figure 6 shows the results from B15; position 12 is the highest, being nearly opposite the windward direction, and just shows a gradual decrease in the correlation with increasing time lag. 30° round, at position 11, there is very poor correlation because this transducer was experiencing alternating pressure and suction. Positions 8, 9 and 10 are all similar to each other showing an initial rapid decrease in the correlation, then they have a 'hump' at about 4 to 5 seconds lag and then another at about 9 to 10 seconds lag, indicating a definite periodicity in the pressures. This would be due to the shedding of eddies from the side of the Tower at this level, and at this particular wind speed the eddy-shedding frequency is close to the natural frequency of the structure (see later section). Finally, position 7 at the back of the Tower shows a good correlation, indicating that the suction is more predictable. The other half of the Tower (positions 1 to 6) is not shown, the results from the symmetrical positions being almost identical.

Figures 7 (B3 level) and 8 (D3 level) show the same basic characteristics as B15. In particular there are small humps in the curves at the same time lags, and the windward transducer (position 12) is almost identical in each case. There is, however, a slightly greater initial drop in the correlation for the other five transducers (7 - 11) on B3 and D3 as compared with B15.

A typical set of pressure spectra for all nine levels on the windward side of the Tower is shown in Figure 9. The nine curves are not identified since no apparent trend or particular order could be seen in any of the records 1 to 9. For comparison purposes, Davenport's free wind-speed curve is reproduced. In general the spectra show a similar trend to each other, namely that of decreasing variance with increasing frequency, and this is similar to the wind-speed curve.

Figure 10 shows the results from vertical scan 9 of the same record, ie at a position 30° around the Tower. There are now some noticeable peaks in the middle of each spectrum, and the particular floor is identified on each one. The features are explained in relation to vertical scan 10 (Figure 11).

Position 10 is very close to the separation point, and the peaks in the spectra represent the strong periodicity in the variation of the pressure measurements and hence the shedding of eddies. The relative magnitudes of the variance at the frequency of these peaks are different at each level; B3 and B5 are low, B11, B13, B15, D3 and D6 are slightly higher and are about the same as each other, and B9 and B7 are very high. These last two are in the middle of the B-floors on the Tower and are therefore more free from any 'end effects' and turbulence.

The peaks occurred at different wave numbers at each level when based on \bar{V}_{195} , and clearly this was not the local mean speed that occurred. The position of these peaks was then recalculated (Figure 12) using the Meteorological Office information on the variation of wind speed with height⁸. Estimates of \bar{V}_H were obtained, based on a 0.17 power law and a zero-plane displacement of 35 m. This then brought the wave numbers at the peaks in the spectra to between 0.0092 and 0.0117 m^{-1} , with a mean value of 0.0100 m^{-1} . In fact the frequencies at which these peaks occurred are gradually increasing with increasing height and this is consistent with the increase in mean velocity. By using the relationship $S = \frac{n \cdot D}{\bar{V}}$ where n is

the eddy-shedding frequency, \bar{V}_H is the mean velocity at height H, D is the diameter of the structure and S is the Strouhal number, values of S were calculated for each level. There are slight variations in the individual values, the mean value being $S = 0.16$. This is lower than might normally be assumed for the structure, possibly indicating that the mean velocity at each level is too high. As already stated, these velocities were based on variations from \bar{V}_{195} and could be inaccurate.

Figures 13, 14 and 15 show some typical pressure spectra indicating the variations that occur between the different transducers around the Tower at D3, B15 and B3 levels respectively.

As with the autocorrelations, only half the transducers (positions 7 - 12) are shown, the other six being similar. At all three levels similar characteristics can be seen, although they are more noticeable on B15 and D3 than they are on B3. The windward transducer (12) shows a gradual decrease in the variance going towards the higher frequencies, without any marked peaks. The transducers on the side of the Tower (8, 9 and 10) show a peak, as in the spectra from the vertical scans, although this is not so regular on B3. Position 11 is more like position 10 on B3 and D3, but like position 12 on B15. This indicates that position 11 is mainly in the pressure lobe on B15, but in the separated region on the other floors, and this is attributed to a slightly different mean direction at D3, and to the more turbulent flow around B3 which causes departures from the distribution of mean pressures that is found at other levels. Channel 7, at the back of the Tower, also shows a slight difference at each level. On B15 the variance shows no particular peaks, whereas on B3 and D3 the plot is similar to that of position 8, with a noticeable peak, again indicating that at both these levels there is a greater variation in the pressure values even at the back of the Tower.

Structural loads

Total horizontal loads were computed for a 1 m high slice of the Tower at each of the four levels where there was a complete ring of pressure transducers (D3, B15, B7 and B3). A typical set of maximum loads (record 16) that occurred at each level (not necessarily simultaneously) is shown in Table 2. As well as the load averaged over the various durations, the resultant direction of each load is also shown and then the values of the ratios $\text{load}_t \text{ seconds} : \text{load}_{60} \text{ seconds}$ are given.

The first observation concerns the variation of load with height. For mean loads (say 60 second average) there is an increase in load with increasing height, as would be expected from the vertical variation of mean wind speed. It has, however, been shown previously^{1,4} that the gust speeds at lower levels could exceed those at higher levels, and in Table 2 it can be seen that the loads averaged over 1, 2, 3 or even 5 seconds do show an increase at lower levels. This means that at some time during the record the turbulence created by the approaching flow over London caused higher intensity loading on lower levels of the Tower as compared with higher levels. This can be seen graphically in Figure 16, where the loads from Table 2 are plotted.

An inspection of the maximum 3-second loads that occurred for ten records (Figure 17) shows that in general this increase in load with decreasing height was recorded. It can be seen, however, that if measurements had been made at greater heights, then there would probably have been an increase in load above 150 m. In fact some of the records were already showing this trend at the 150 m level.

In comparing Figure 17 with Figures 18 and 19 (Figures 6 and 7 in reference 1) there appears to be a discrepancy between the results, since the pressures on the windward side of the Tower increase with increasing height, whilst the loads, integrated around the structure, increase with decreasing height. The explanation is that although the windward pressure increased with height, the high suction values that occurred around the leeward half of the structure at lower levels were a major factor in determining the total loads. This can be seen from Figure 20, which shows the 3-second pressure distribution around the Tower at each level at the time when the maximum 3-second load occurred on each floor. In this particular record the maximum loads occurred simultaneously on all levels; this was not always the case, but even when the peak loads occurred at different times at each level, the same overall pattern, of increasing windward pressure and decreasing leeward suction with increasing height, was observed.

It was previously reported¹ that a typical value of the force (drag) coefficient for the Tower was 0.63. As further analysis has now been carried out, more detailed results can now be given. The maximum 3-second loads for each record (Figure 17) can be converted to force coefficients, C_f , based on the peak gust velocity at the top of the tower, \hat{V}_{195} . The averages of these 3-second C_f values from all the records were 0.57, 0.60, 0.75 and 0.85 at heights of 152 m, 104 m, 67 m and 49 m respectively.

The way in which the short duration gusts affected the instantaneous loads on each floor can be seen by the second-by-second plots of the (1-second) load vectors (Figure 21). A 20-second period of the results from all four floors is shown, the mean wind direction at 195 m for this period being 345° and the wind speed being $24 \pm 2 \text{ m/s}$.

The striking observation is the difference between the vectors from D3 and B15, and those from B7 and B3. In both direction and magnitude there is much less variation on the upper floors, corresponding to the less turbulent wind at higher levels. However the turbulence at lower levels causes a large scatter in both the direction and magnitude of the resultant loads. In fact as mentioned previously, the loads on B3 and B7 are much greater than those on B15 and D3.

A significant factor in determining structural loads for design purposes is the size of gusts in relation to the size of the structure. The gust sizes, as experienced by the structure, can be determined by correlating the pressures measured at two separate points. The cross-correlation function is a measure of the information which is given by the instantaneous value of the pressure at one point about the value of the pressure at the other point, and at a time t seconds later. For zero time lag, the cross-correlation is therefore a measure of the relationship between simultaneous values of the pressures at different points.

For each record, cross-correlations were computed between pairs of transducers and a typical set of squares of correlation coefficients at zero lag, r^2 , is given in Table 3 for a vertical scan on the windward side of the Tower. Use of the heights in Figure 2 enables the r^2 values to be plotted against the particular separation distance, and a plot of the results from this same record is shown in Figure 22. It can be seen that, even for transducers separated by up to 120 m, there is quite a high overall correlation of the pressure signals.

To see if this was also the case at different positions around the structure, the results for vertical scans 9 and 10 of the same record are indicated in Figure 23. The coefficients on the windward side of the Tower (position 8) have again been included for comparison, all three sets being drawn as a broad band rather than individual points. Moving around the Tower 30° showed a decrease in the correlation to some extent, although for this particular record it was still quite high at 120 m. (Some records were like this, others had r^2 values at 120 m of approximately 0.1.) Another change of 30° to position 10 reduced the correlation still further, r^2 now being approximately zero at about 60 m separation.

Values of the square root of the coherence were calculated and plotted against the reduced frequency nX/\bar{V} as, for example, in Figure 24. The best-fit exponential decay curve was determined in each case, as Davenport suggested¹⁰ that the $\sqrt{\text{coherence}}$ can be expressed in the form $\sqrt{\text{Coherence}} = e^{-CnX/\bar{V}}$. From all the correlations considered, the mean value of the constant C was 6.8 with a standard deviation of 1.8. This is higher than was found at Royex House⁵, and in fact approaches the generally accepted value of 7.7 for eddies in the free wind.

All the individual C values are plotted in Figure 25 against the vertical separation between the relevant pair of transducers. It can be seen that the results from the transducers that were 9 m and 10 m apart are slightly higher than the rest. In fact for the 9 m and 10 m results, the mean value of C was 8.4 with a standard deviation of 1.9, whereas for the rest of the results the mean value is 6.1 with a standard deviation of 1.3. Therefore the 9 m and 10 m results have an influence on the overall mean, changing it from 6.1 to 6.8. A high C value (eg 8.4) would imply a smaller effective gust width, but as coherence is plotted against the reduced frequency, which takes account of the spatial separation, it might be expected that there should be no significant variation in the results at any separation.

Harris¹¹ has shown that, within limitations, Davenport's formula for coherence is consistent with a more rigorously derived expression based on the case of homogeneous isotropic turbulence. It was considered that this expression might provide a better fit to the Tower data and hence explain the different C values at the small separation distances between transducers. However, there is a considerable range of decay curves, based on the various values of the constant C , each of which is the best fit for the particular set of data. In Figure 26 four such curves ($C = 4, 6, 8$ and 10) are shown, together with the Harris curve which is based on Bessel functions.

There is no constant in Harris's expression which can alter the slope of the curve for different sets of data. Therefore this more rigorously derived expression, whilst fitting a few of the Tower results, is a worse fit for many of them, and does not provide the answer to the problem. Davenport¹² has recently suggested that the variation in C values might not be excessive as a considerable range of transducer positions and local velocities are combined in Figure 25. Further analysis of the results will be carried out shortly.

Strain measurements

The final analysis that was carried out concerned the oscillations of the Tower as detected by the strain gauges on the reinforcing bars at the A8 level (29 m). Before the records were taken, all channels were balanced in order to remove any mean drift due to a long-term movement of the Tower (eg because of solar heating). Therefore all the results concern the dynamic strain about the mean position at the beginning of the record.

A visual inspection of the records proved useful as a first stage of the analysis. (Part of a record is shown in the Appendix, Figure A2.) All twelve strain gauges oscillated about their deflected mean position, part of the time being relatively quiet with only small oscillations but for most of the record showing a considerable amplitude to the oscillations. The quiet periods did not necessarily coincide with lulls in the wind speed, neither did the maximum movement coincide with the gusts. Both these observations would suggest that any change in amplitude, due to a sudden change in wind speed, occurred over a period of several cycles. The time period for the oscillations indicated that the natural frequency of the structure was 0.157 Hz. This visual inspection also indicated that the direction of oscillation of the Tower most of the time was nearly perpendicular to the wind direction.

After this visual inspection the records were converted to a digital form, in the same way as the pressure records, prior to computation. A typical instantaneous strain distribution recorded by all twelve gauges can be seen in Figure 27. Part of the circumference is in compression and the rest is in tension (relative to the mean position), and this situation changed in cycles, as was indicated from the visual inspection. Peak levels of strain did not necessarily occur at peak gust speeds; typically the peak dynamic strain was of the order of 25×10^{-6} . Rms values for both records, averaged over the length of the record, were typically about 6×10^{-6} .

Autocorrelation functions were determined for all gauges, and for record 17 these are shown in Figure 28. It can be seen that at all positions around the Tower, the strain can be well predicted at time lags of about $6\frac{1}{2}$, 13, $19\frac{1}{2}$ etc seconds, as the autocorrelations show a very strong periodicity (ie the natural period of the Tower). The mean wind direction at 195 m was approximately opposite position 3, and it is noticeable that gauges 3A8 and 9A8 (windward and leeward sides of the Tower) show smaller fluctuations in the autocorrelations of the strain than the side gauges (which were experiencing alternate tension and compression) where the autocorrelation function varied between +1.0 and -0.8 in some cases.

Strain spectra for the variance of two gauges are shown in Figure 29. The results from all twelve gauges in both records show a very narrow-band peak for the normalised strain spectrum, centred about a frequency of 0.157 Hz. This confirms the estimate based on the visual inspection of the records, and corresponds to a natural period of vibration of 6.37 seconds. It also agrees with the estimated value (0.16 Hz) when the Tower was designed¹³.

Although all the spectra indicated the same frequency for all the peaks, the magnitude varied according to the position around the Tower, as given in Table 4 (for record 17). This confirms the observations from the autocorrelations, where the side gauges were seen to have the greatest variance, gradually decreasing around the Tower towards the windward and leeward gauges, where there was the least variance.

In the same way that the pressure measurements were combined to give the resultant load vector on each floor, so all twelve strain measurements were combined to give the resultant bending moment vector, eg as shown by the arrow in Figure 27. Some typical plots of the second-by-second position of these vectors are shown in Figures 30-33, for periods of between 20 and 25 seconds. The points indicate the position at each 1-second interval, and the arrows represent the range of wind directions for the short period considered.

These diagrams are based on the vertical dynamic strain in the reinforcement at 29 m above ground level. They represent the bending moment at that height, and if it is assumed that the Tower oscillated as a simple cantilever in a single mode, then the diagrams are representative (to some unknown scale) of the horizontal movement of the top of the Tower.

For the majority of both records, the Tower oscillated transversely to the mean wind direction as can be seen in Figure 30. There were, however, variations in this pattern. For instance, occasionally there was a change in direction (Figure 31) for a short period, possibly due to severe gusts on part of the structure. There were also times when the mean position had apparently changed from the beginning of the record (Figure 32). This figure also indicates a period when the oscillations were not exactly transverse to the wind direction at 195 m. Finally, Figure 33 shows an occasion when the movement had decreased considerably, and the direction of oscillation was extremely indeterminate. This was a

period when the wind speed had decreased; this is confirmed by the mean position of the vector, which is towards the mean wind direction as compared with the beginning of the record. The situations in Figures 31-33 can obviously occur, but the main movement was as shown in Figure 30.

DISCUSSION AND CONCLUSIONS

The relevance to design of the results that concern cladding loads cannot be finally assessed until the analysis of the open-scale records has been finished. Gust factors based on these short duration pressures will be presented and discussed at the same time.

Variations can be seen in the autocorrelations for different positions around the Tower, and also at different levels. They do not show any unexpected results, the least correlated pressure signals coming from transducers in positions of greatest turbulence.

It is shown that the pressure spectra on the windward side of the structure are of a similar shape to that of the free wind. This indicates that most of the variance in these pressure measurements comes from the turbulence in the approaching wind flow. However, this situation gradually changes around the Tower, and at 60° from the wind direction very large peaks can be seen in the spectra indicating regular fluctuations in the pressures. At the range of wind speeds at which the records were taken, the frequency of these fluctuations (due to the eddy shedding from the side of the structure) was typically 0.1 Hz at the bottom levels increasing to 0.2 Hz at the top. This is not within the range of natural frequencies of the cladding panels and is therefore unlikely to lead to cladding resonance, but it does confirm the importance of relatively short duration gusts for cladding loads. The further analysis of open-scale records could indicate other peaks in the spectra at higher frequencies, as it is thought that there are considerable pressure variations on some transducers due to turbulence created by the mullions etc.

The vertical variation of the total horizontal loads shows greater loads at lower heights for short duration averaging times. Similar results were obtained from the 118 m high Vickers Tower, Millbank¹⁴, and also, to some extent, from the Tokyo Tower¹⁵. The main reason for this occurring at the Tower is the magnitude of the short duration suctions on the leeward half of the structure at the low levels. The loading gust factors (eg those shown in Table 2) that result from these high loads are very important when considering the design of such a structure, and they are not normally taken into account.

The size, and hence duration, of gusts that should be used for design purposes, based on the pressure correlations between pairs of transducers, has previously been discussed¹. It was indicated that, using the British wind loading Code of Practice, CP3, Chapter V, Part 2, 1972, an under-estimate of the required gust duration could still be made. Ideally an exact gust duration could be calculated based on the equation $t = C \cdot D / \bar{V}$ seconds; C is given as 6.8 in this paper, or 4.4 from Royex House⁵, the latter being a broad-fronted slab office block. The calculation of t may be an iterative process, as the selection of the design wind speed itself depends to some extent on a knowledge of the gust duration, but this is seen as a surmountable problem with the use of computer programs for design. However, if a stepped progression of gust durations for various sizes of structures is required rather than the above equation, the following are recommended:

- 3-second gust for buildings up to 30 m
- 5-second gust for buildings from 30 m to 50 m
- 10-second gust for buildings from 50 m to 100 m
- 15-second gust for buildings over 100 m

all these lengths applying to either the largest horizontal or vertical dimension of the structure. To implement this one would need an amendment to CP3, Chapter V, but it is considered that these recommended gust durations would lead to more accurate design loads.

The dynamic movement of the Tower, as detected by the strain gauges, was at a frequency of 0.157 Hz and, at the range of wind speeds at which recordings were made, most of this movement was transverse to the mean wind direction. Unfortunately comparisons could not be made of the in-wind and across-wind deflections for a wider range of wind speeds.

Other full-scale tests have been carried out on tall slender structures, and the oscillation results of these tests can be compared with the results in this paper. Ishizaki¹⁶ tested an 80 m high all-welded steel tower in Kyoto, with a fundamental natural period of 1.3 seconds, and gives a plot of the movement of the top of the structure. It is shown to move in an elliptical fashion with the minor axis of the ellipse (in-wind direction) approximately half the major axis (cross-wind direction) for winds up to about 25 m/s and also above 35 m/s. In between these speeds the amplitude perpendicular to the wind direction increases considerably, giving a similar movement to that shown in Figure 30. Van Koten¹⁷ reports

some measurements made on a 100 m high cylindrical tower. This again agrees with the Post Office Tower results, as he found that the transverse vibrations were much larger than the vibrations in the wind direction, the ratio between the two amplitudes being about 4:1.

At the Post Office Tower itself, some measurements were taken directly of the displacement of the top of the Tower by W C Ramsay of the (then) Ministry of Public Building and Works¹⁸. This was done by installing a gyro unit, which recorded the magnitude and direction of the deflection, at the centre of the top of the Tower. Ramsay states that there were many problems with the equipment and that relatively few useful results were obtained; also the anemometer at 195 m was not used for the wind data as it did not cover the full period of the tests. Instead meteorological information was used from the London Weather Centre. Plots are given of the resultant movement of the top of the structure; some are elliptical but others cross over themselves like a figure-of-eight and some are irregular curves with 'kinks', said to be due to the influence of the bridge link to the adjacent telephone exchange building.

The authors would like to see further measurements made on this aspect of the work. All the strain gauges and their connections at level A8 are still in existence, as is the anemometer at 195 m, and new equipment is now available to measure deflections very easily, provided a line of sight is available. Such measurements at the Tower would enable velocities, deflections and resulting strains to be measured simultaneously.

ACKNOWLEDGEMENT

The authors wish to thank the Post Office authorities for allowing the use of the Tower for this project, and also members of staff of the (then) Ministry of Public Building and Works for their assistance during the installation of the equipment.

The work described has been carried out as part of the research programme of the Building Research Establishment of the Department of the Environment.

REFERENCES

- 1 Newberry, C W, Eaton, K J and Mayne, J R. Wind pressures on the Post Office Tower, London. Proceedings of the 3rd International Conference on Wind Effects on Buildings and Structures, Tokyo, September 1971. (BRS Current Paper CP37/71.)
- 2 Eaton, K J and Mayne, J R. Strain measurements at the GPO Tower, London. Strain, Vol 7, No 3, July 1971, pp 103-109. (BRS Current Paper CP29/71.)
- 3 Eaton, K J and Mayne, J R. Instrumentation and analysis of full-scale wind pressure measurements. NPL Symposium on Instrumentation and Data Processing for Industrial Aerodynamics, 1968. (BRS Current Paper CP1/69.)
- 4 Eaton, K J. Wind loading on tall buildings. PhD Thesis, University of London, 1972.
- 5 Newberry, C W, Eaton, K J and Mayne, J. R. Wind loading on tall buildings - further results from Royex House. Industrial Aerodynamics Abstracts, Vol 4, No 4, July-August 1973. (BRE Current Paper CP29/73.)
- 6 Bendat, J S and Piersol, A G. Measurement and analysis of random data. New York, Wiley, 1966.
- 7 Shellard, H C. Results of some recent special measurements in the United Kingdom relevant to wind loading problems. International Seminar on Wind Effects on Buildings and Structures, Ottawa, 1967, pp 515-533.
- 8 Helliwell, N C. Some open scale measurements of wind over Central London. World Meteorological Office Symposium, Brussels, 1968, pp 46-48.
- 9 Helliwell, N C. Wind over London. Proceedings of the 3rd International Conference on Wind Effects on Buildings and Structures. Tokyo, September 1971.
- 10 Davenport, A G. The relationship of wind structure to wind loading. Proceedings of the 1st International Conference on Wind Effects on Buildings and Structures. NPL, Teddington, 1963, pp 53-102.

- 11 **Harris, R L** The nature of the wind. Paper 3, CIRIA Seminar, The modern design of wind-sensitive structures, June 1970, pp 29-55.
- 12 **Davenport, A G**. Private communication.
- 13 **Creasy, L R, Adams, H C and Lampitt, N**. Museum Radio Tower, London. Proceedings of the Institution of Civil Engineers, Vol 30, 1965, pp 33-78.
- 14 **Newberry, C W, Eaton, K J and Mayne, J R**. Wind loading on Vickers Tower, Millbank. Building, Vol 219, No 6639, August 1970, pp 53-56. (BRS Current Paper CP35/70.)
- 15 **Arakawa, H and Tsutsumi, K**. Strong gusts in the lowest 250m layer over the City of Tokyo. Journal of Applied Meteorology, Vol 6, 1967, pp 848-851.
- 16 **Ishizaki, H**. Effects of wind pressure fluctuations on structures. International Seminar on Wind Effects on Buildings and Structures, Ottawa, 1967, pp 265-277.
- 17 **Van Koten, H**. Vortex excitation. Proceedings of the Conference on Tower-Shaped Structures, The Hague, 1969, pp 115-143.
- 18 **Ramsay, W C**. Private communications.

Table 1 Details of records at the Post Office Tower

Record no.	Date	Time GMT	Mean direction	\hat{V}_{195} (m/s)	\bar{V}_{195} (m/s)	T (seconds)	Transducers used									
							B 3	B 5	B 7	B 9	B 11	B 13	B 15	D 3	D 6	Strain
1	16.10.67	18.07	203 ^o	25	18	400	3	3	3	3	3	3	3	3	3	-
2	17.10.67	00.07	209 ^o	27	20	400	3	3	3	3	3	3	3	3	3	-
3	17.10.67	03.07	222 ^o	28	20	400	3	3	3	3	3	3	3	3	3	-
4	17.10.67	04.07	193 ^o	33	25	400	3	3	3	3	3	3	3	3	3	-
5	17.10.67	05.07	195 ^o	30	21	400	3	3	3	3	3	3	3	3	3	-
6	17.10.67	06.07	219 ^o	26	19	400	3	3	3	3	3	3	3	3	3	-
7	17.10.67	07.07	213 ^o	27	19	400	3	3	3	3	3	3	3	3	3	-
8	15. 1.68	12.51	265 ^o	22	15	1200	3	3	3	3	3	3	3	3	3	-
9	15. 1.68	13.15	265 ^o	21	16	120	3	3	3	3	3	3	3	3	3	-
10	6. 3.68	17.34	325 ^o	32	22	1200	12	-	12	-	-	-	12	11	-	-
11	20. 3.68	13.12	225 ^o	25	15	800	12	-	12	-	-	-	12	11	-	-
12	20. 3.68	16.27	210 ^o	30	20	1200	12	-	-	-	-	-	12	11	-	-
13	20. 3.68	23.03	205 ^o	20	21	1200	12	-	-	-	-	-	12	11	-	-
14	15.11.68	18.02	70 ^o	18	14	700	12	-	12	-	-	-	12	11	-	-
15	22.12.68	04.16	248 ^o	15	13	1200	12	-	12	-	-	-	12	11	-	-
16	7. 2.69	18.08	244 ^o	28	20	1200	12	-	12	-	-	-	12	11	-	-
17	19. 2.69	14.24	68 ^o	20	14	1200			12	-	-	-	12	11	-	12
18	19. 2.69	15.09	67 ^o	18	13	1200	-	-	-	-	-	-	-	-	-	12
19	12. 4.69	03.35	247 ^o	15	13	1200	12	-	12	-	-	-	12	11	-	-
20	12. 4.69	10.20	263 ^o	19	13	1200	12	-	12	-	-	-	12	11	-	-

Table 2 Variation of load with averaging time

Record 16		$\hat{V}_{195} = 25 \text{ m/s}$				$q(3 \text{ seconds}) = 481 \text{ N/m}^2$			
Floor		Averaging period (seconds)							
		1	2	3	5	10	15	30	60
D3 152m	Load (N) _O	4735	4520	4371	4322	4159	3991	3872	3364
	Angle (°)	176	174	174	173	167	168	169	169
	Load ratio	1.41	1.34	1.30	1.28	1.24	1.19	1.15	1.00
B15 104 m	Load (N) _O	4980	4792	4602	4527	4355	4146	3761	3005
	Angle (°)	169	174	167	168	170	168	168	168
	Load ratio	1.66	1.59	1.53	1.51	1.45	1.38	1.25	1.00
B7 67 m	Load (N) _O	6745	5575	5374	5081	4081	3716	3042	2406
	Angle (°)	206	185	173	170	168	171	174	173
	Load ratio	2.80	2.32	2.24	2.12	1.70	1.54	1.26	1.00
B3 49 m	Load (N) _O	7409	7124	6362	5350	4659	4196	3111	2162
	Angle (°)	161	160	155	156	167	173	172	171
	Load ratio	3.42	3.29	2.94	2.47	2.16	1.94	1.44	1.00

Table 3 Cross-correlations at zero lag

PO Tower
Record 3

(Correlation coefficient)²

8B3	1.00								
8B5	0.68	1.00							
8B7	0.56	0.70	1.00						
8B9	0.50	0.60	0.78	1.00					
8B11	0.35	0.38	0.59	0.71	1.00				
8B13	0.29	0.30	0.49	0.57	0.77	1.00			
8B15	0.28	0.26	0.43	0.50	0.68	0.83	1.00		
8D3	0.26	0.28	0.39	0.38	0.37	0.40	0.40	1.00	
8D6	0.23	0.22	0.32	0.32	0.33	0.36	0.34	0.66	1.00
	8B3	8B5	8B7	8B9	8B11	8B13	8B15	8D3	8D6

Table 4 Variation of the peak value of the strain spectra

Position	$\bar{\theta}$ (relative to the wind)	Peak value of $\frac{n \cdot S_s(n)}{\sigma_s^2}$
1	- 63°	1.93
2	- 33°	1.28
3	- 3° (Windward)	0.45
4	27°	1.44
5	57°	2.22
6	87° (Side)	2.38
7	117°	2.36
8	147°	1.80
9	177° (Leeward)	0.95
10	-153°	2.06
11	-123°	2.64
12	- 93° (Side)	2.65



Figure 1 General view of Post Office Tower

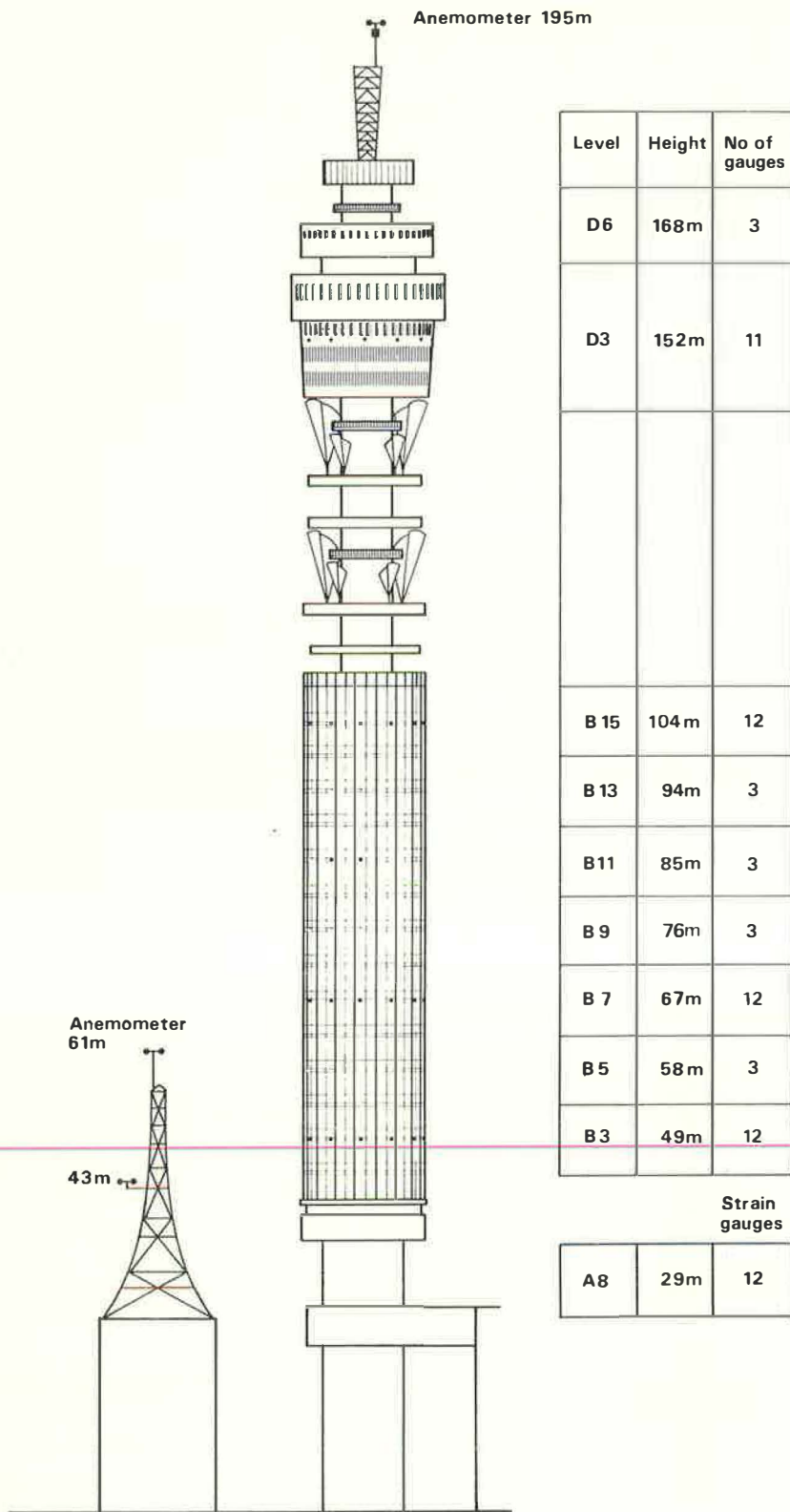


Figure 2 Arrangement of anemometers, pressure transducers and strain gauges

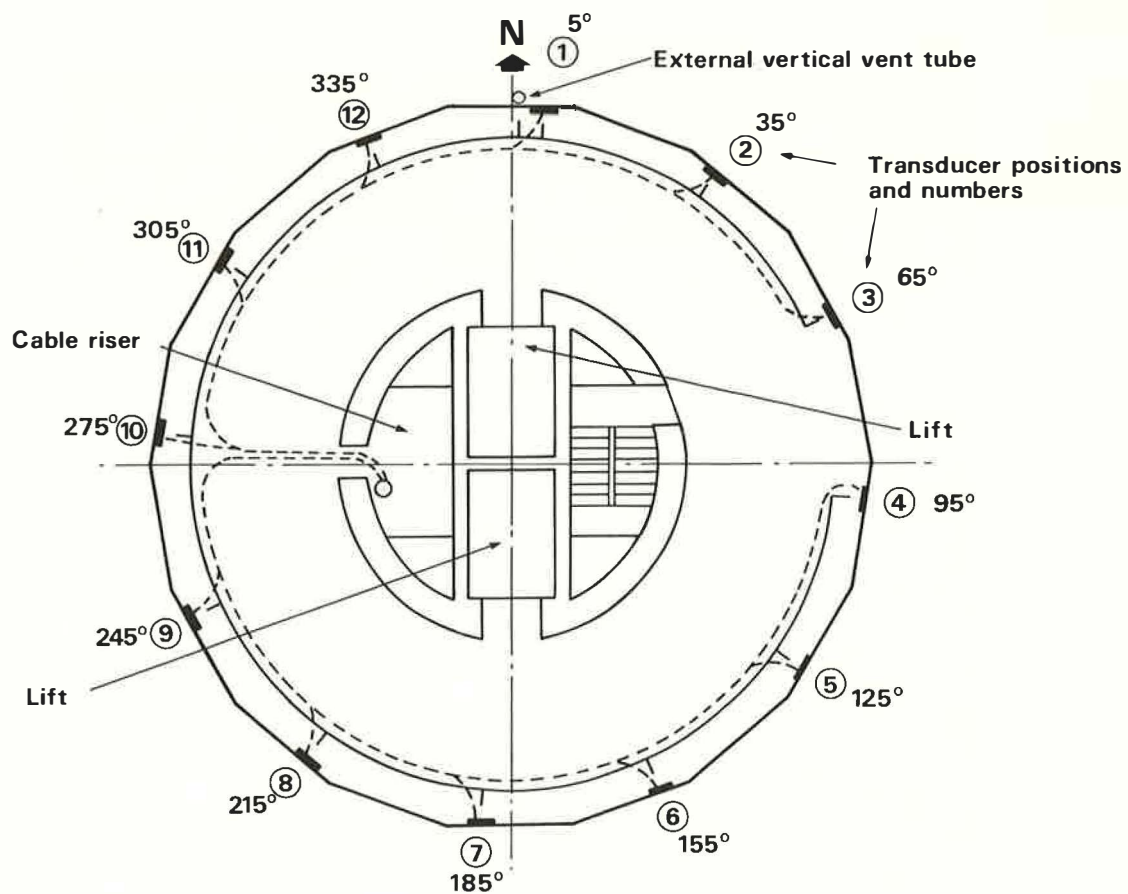


Figure 3 Transducer positions on a B-floor

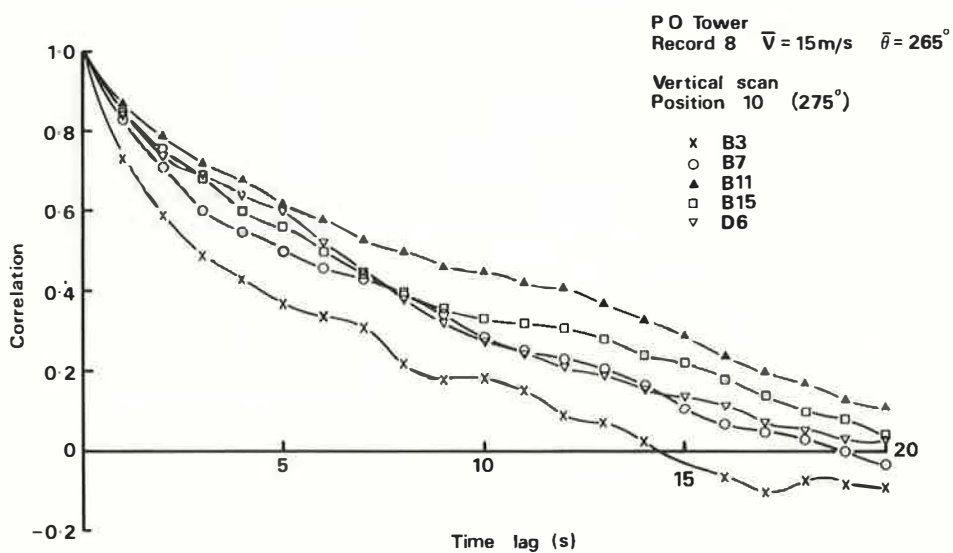


Figure 4 Autocorrelations, vertical scan 10

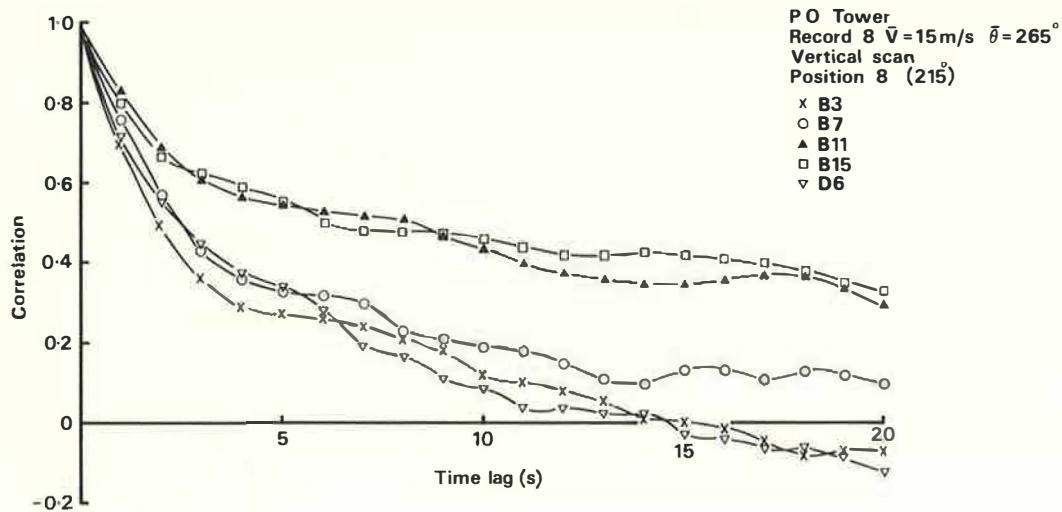


Figure 5 Autocorrelations, vertical scan 8

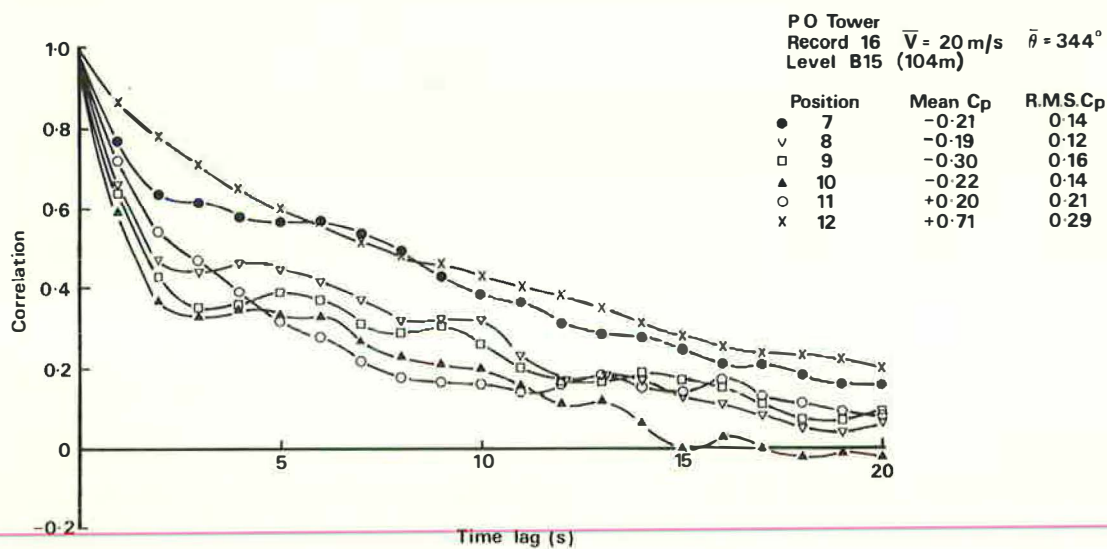


Figure 6 Autocorrelations, level B15

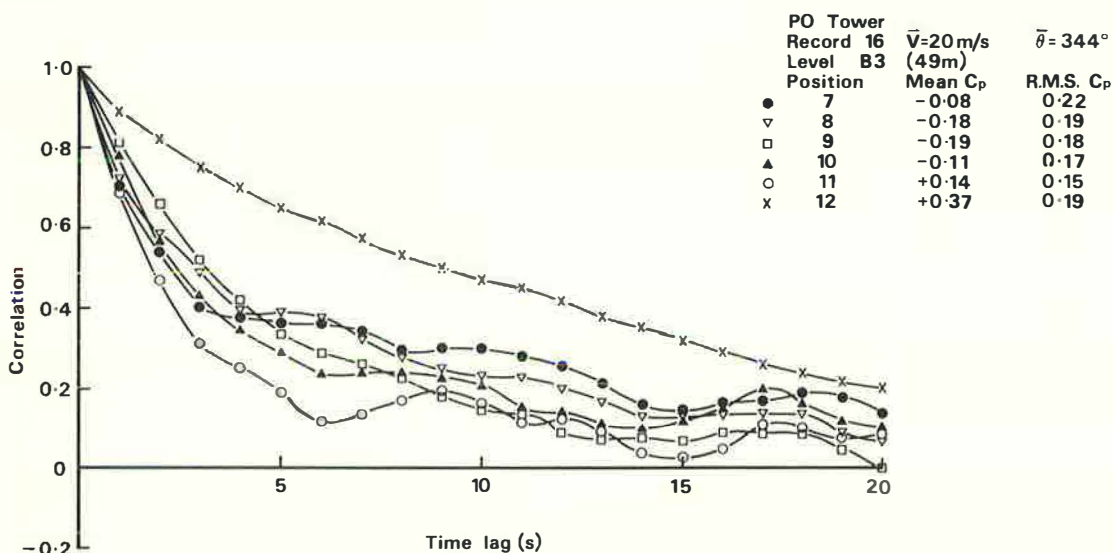


Figure 7 Autocorrelations, level B3

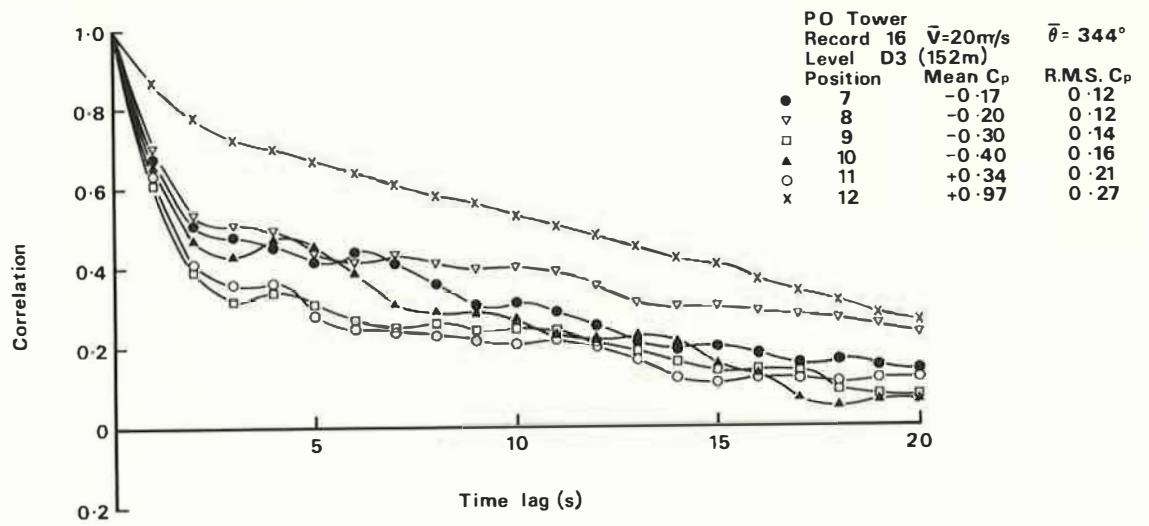


Figure 8 Autocorrelations, level D3

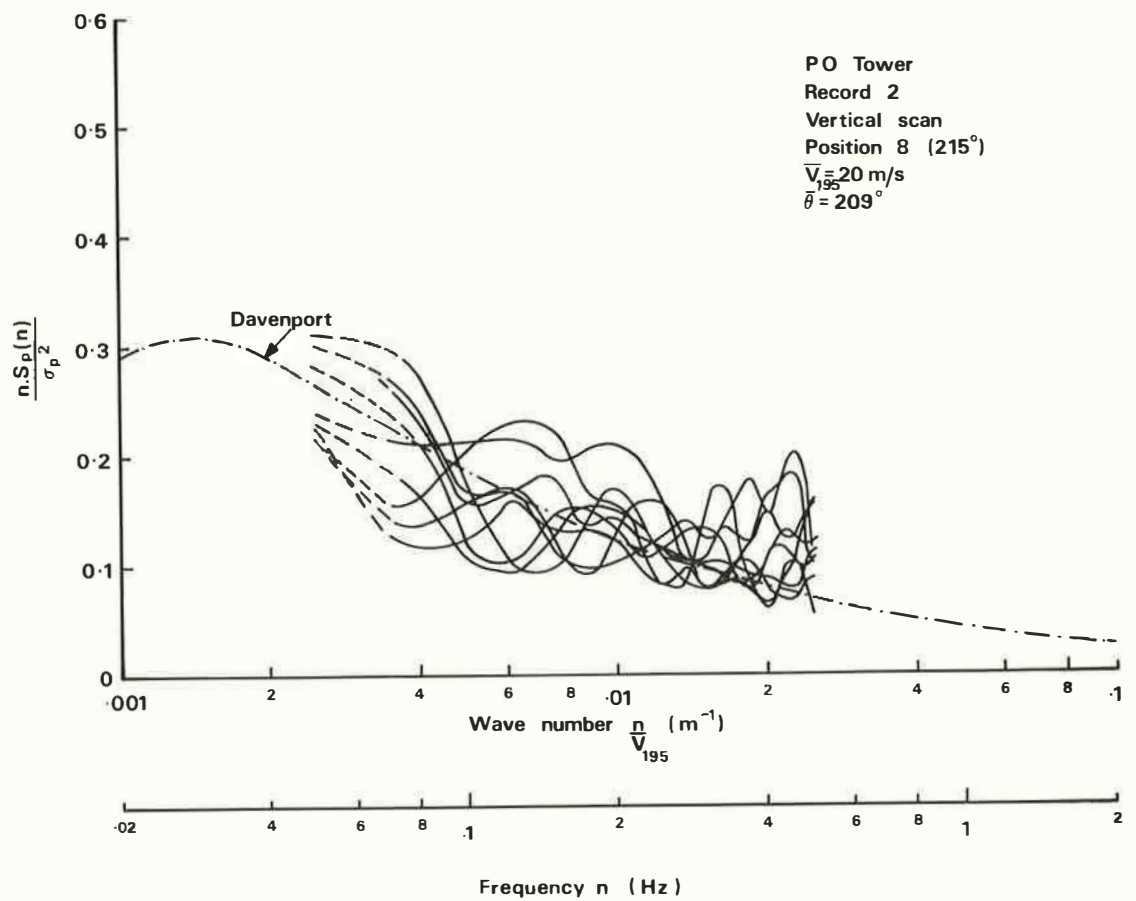


Figure 9 Pressure spectra, vertical scan 8

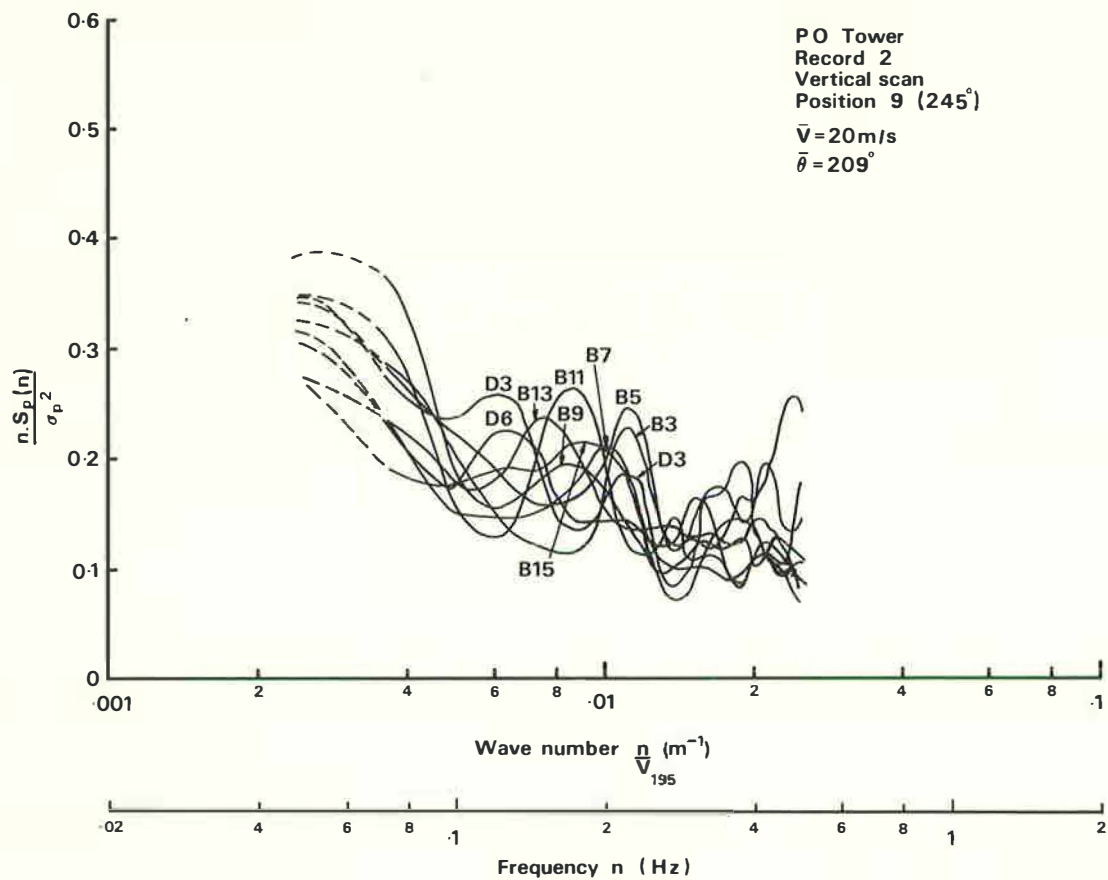


Figure 10 Pressure spectra, vertical scan 9

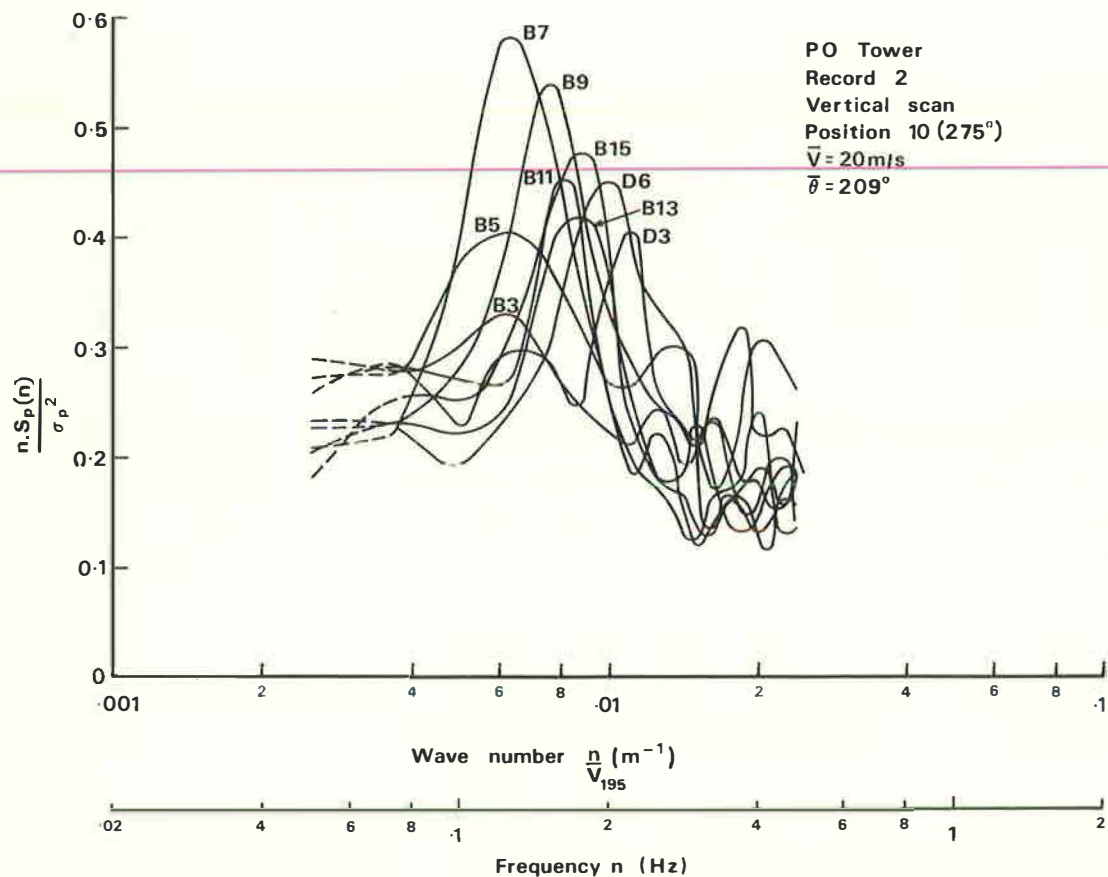
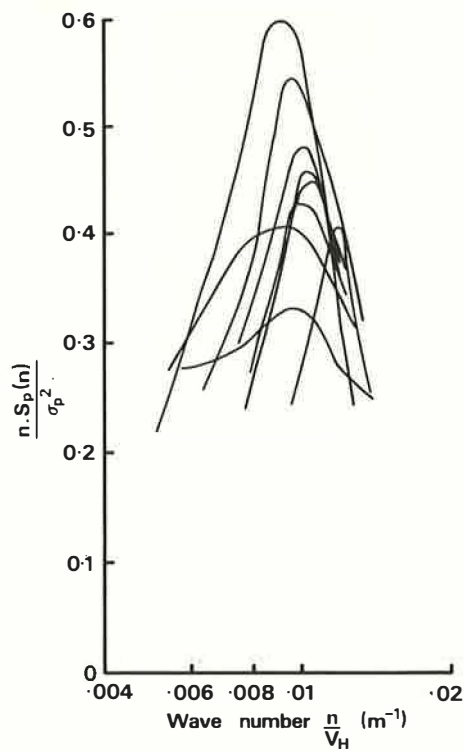


Figure 11 Pressure spectra, vertical scan 10



P O Tower Vertical scan		Record 2 Position 10 (275°) $\bar{V}_{195} = 20\text{m/s}$ $\bar{\theta} = 209^\circ$		
Level	Actual Height H (m)	\bar{V}_H (m/s)	Peak Wave No (m ⁻¹)	Peak Frequency Hz
D 6	168	18.7	.0102	.191
D 3	152	18.3	.0117	.215
815	104	16.8	.0100	.168
813	94	16.3	.0100	.163
811	85	15.9	.0105	.167
8 9	76	15.3	.0096	.147
8 7	67	14.7	.0092	.135
8 5	58	13.9	.0092	.128
8 3	49	12.8	.0097	.124

Figure 12 Peak pressure spectra, vertical scan 10

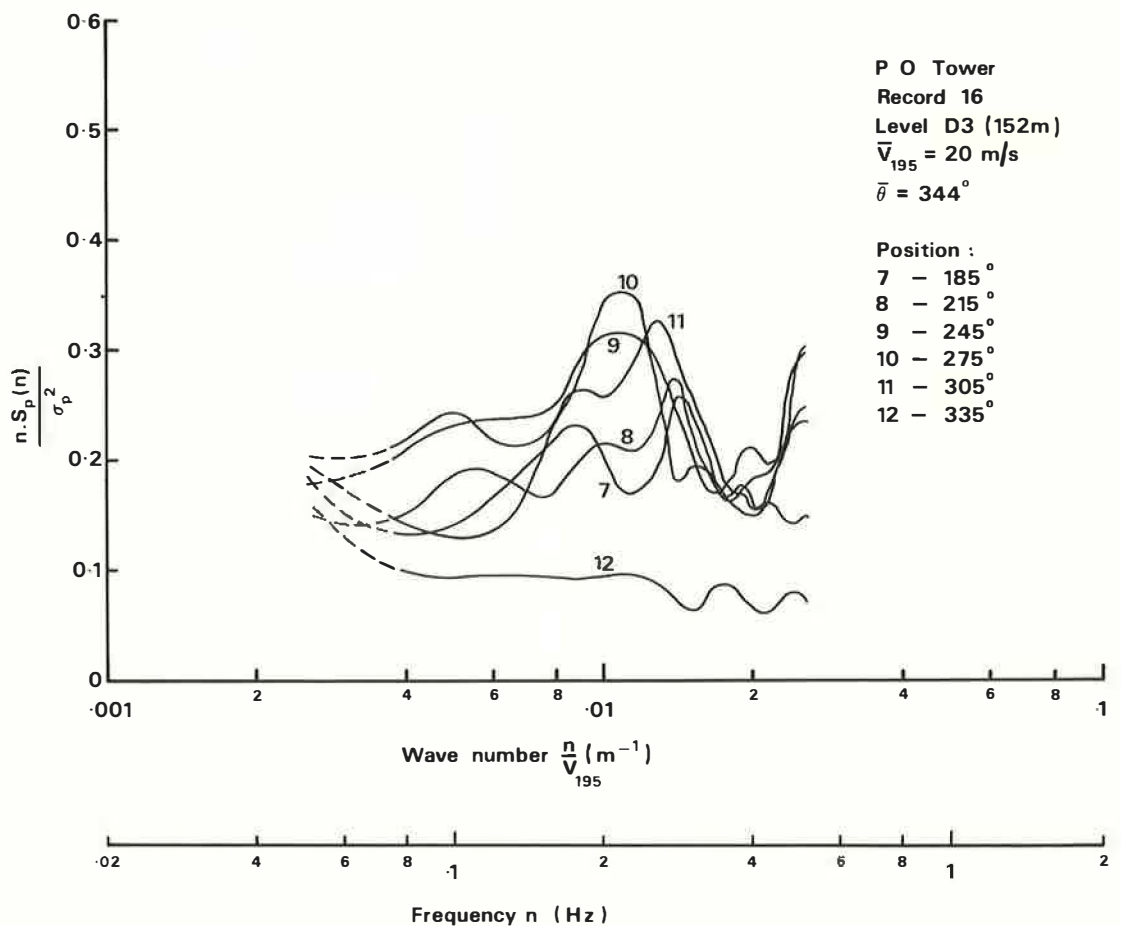


Figure 13 Pressure spectra, level D3

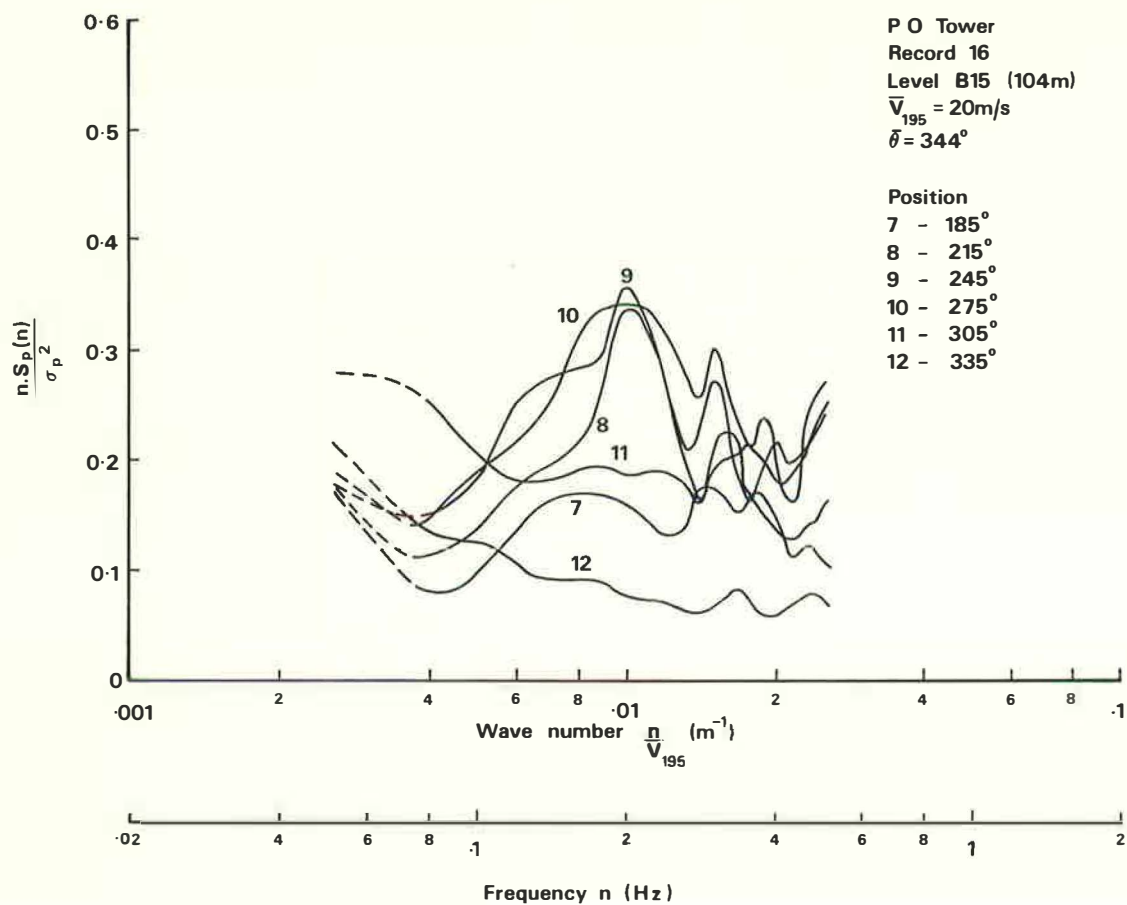


Figure 14 Pressure spectra, level B15

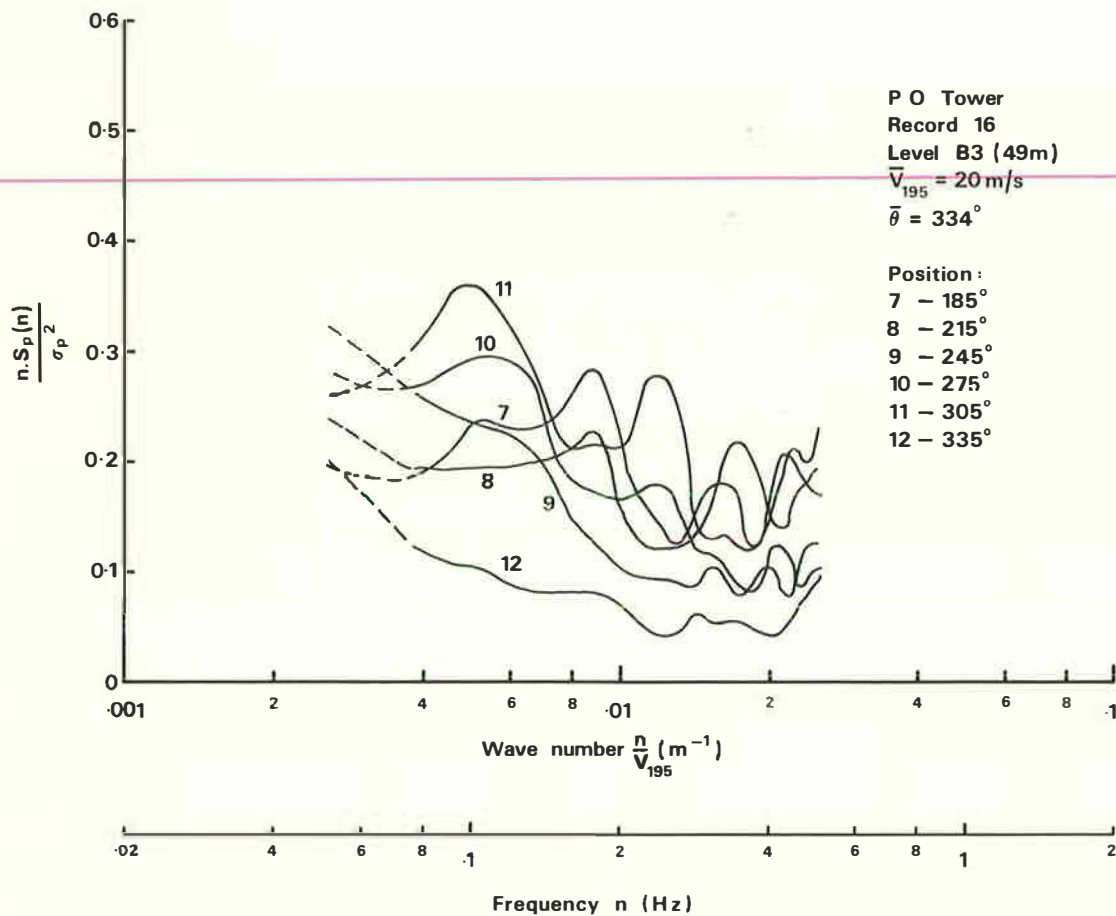


Figure 15 Pressure spectra, level B3

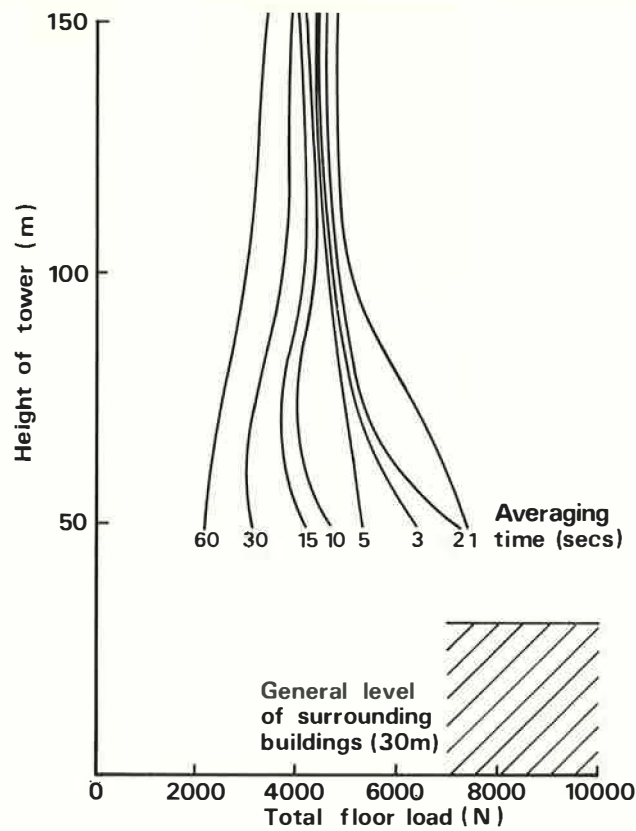


Figure 16 Vertical variation of floor loads

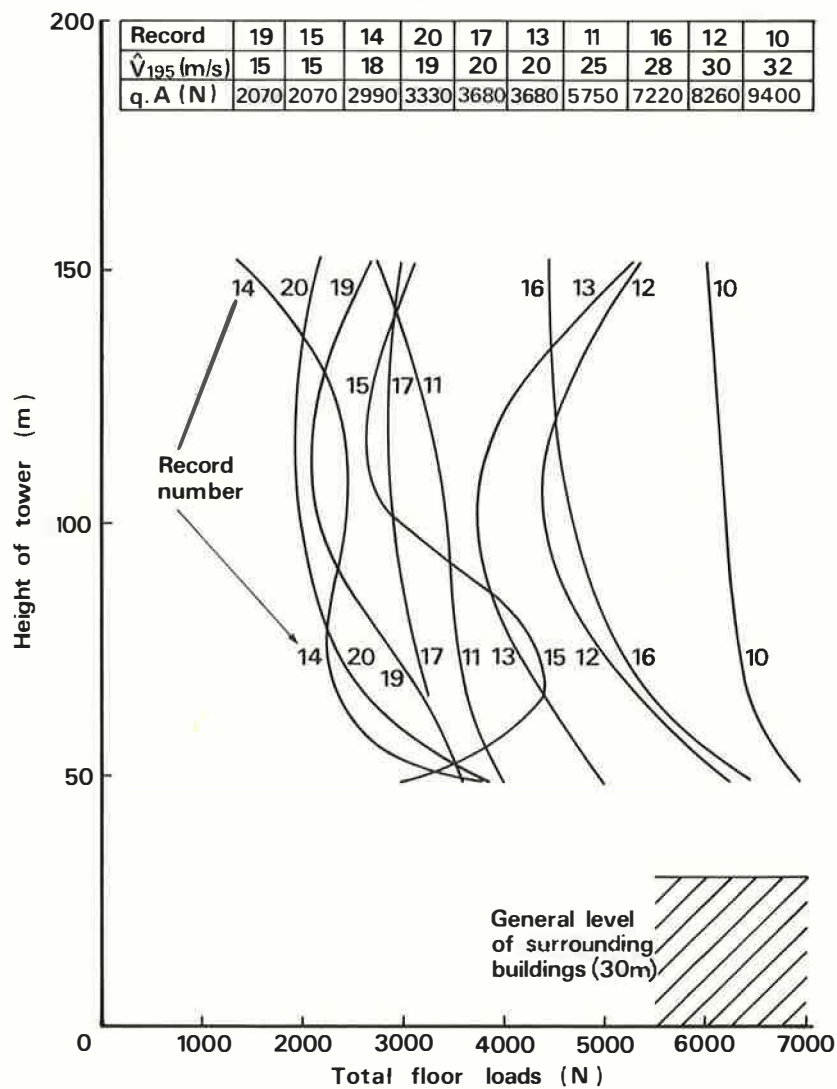


Figure 17 Maximum 3-second loads during each record

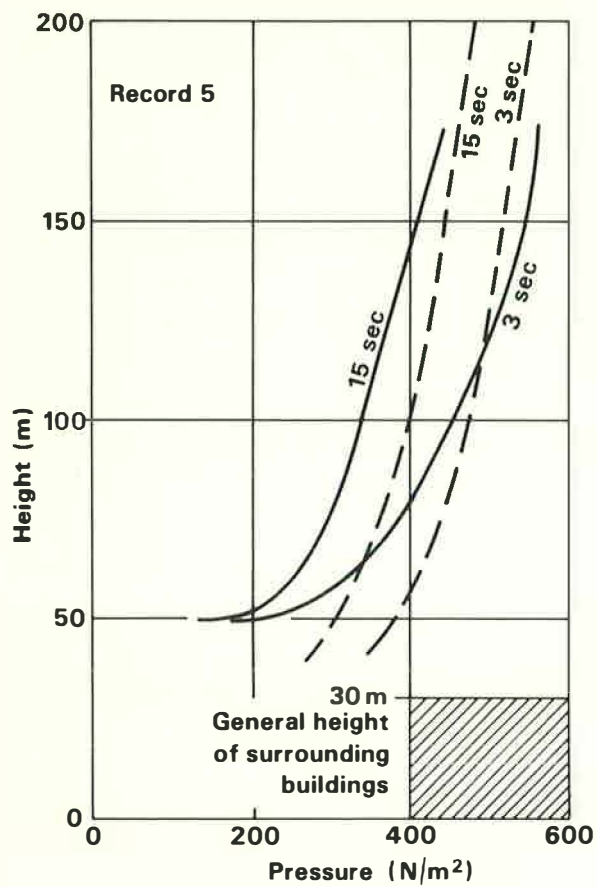


Figure 18 Variation of pressure with height (record 5)

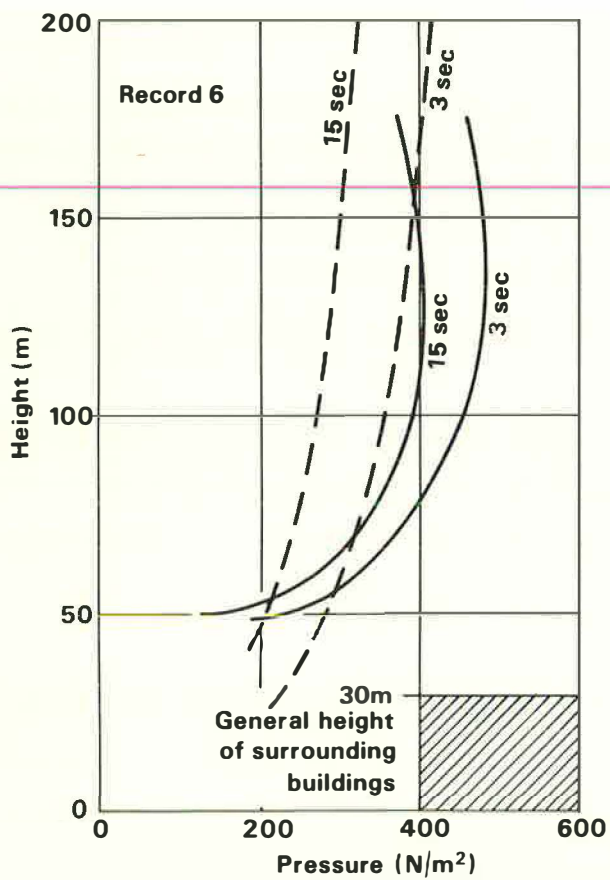
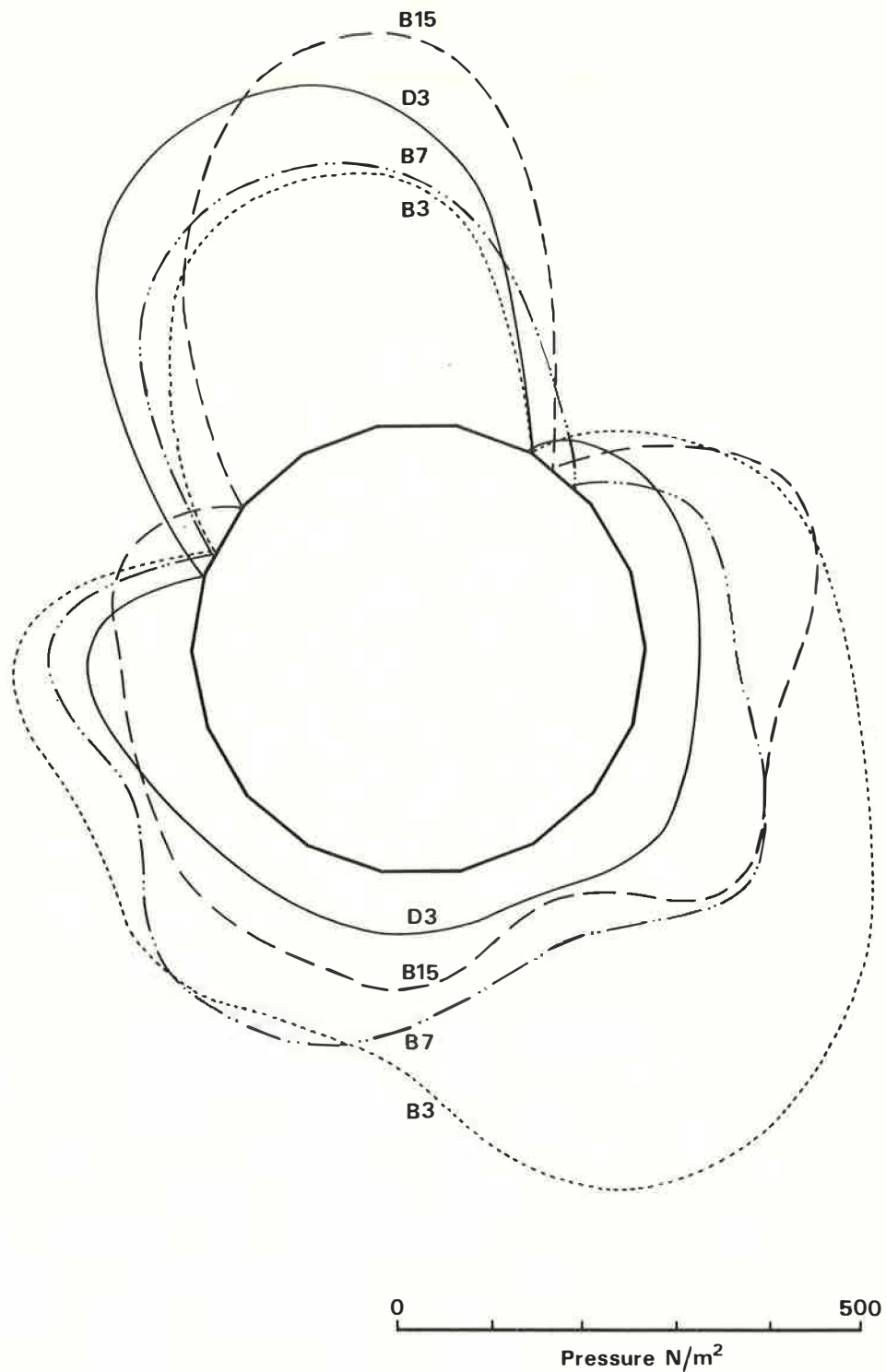


Figure 19 Variation of pressure with height (record 6)



Record 16

	Floor	Height (m)	Load (N)	Angle (deg)
————	D3	152	4276	170
— — — —	B15	104	4602	167
- · - · - ·	B7	67	5374	174
· · · · ·	B3	49	6362	155

Figure 20 (Simultaneous) Maximum 3-second pressures and loads

Record 16

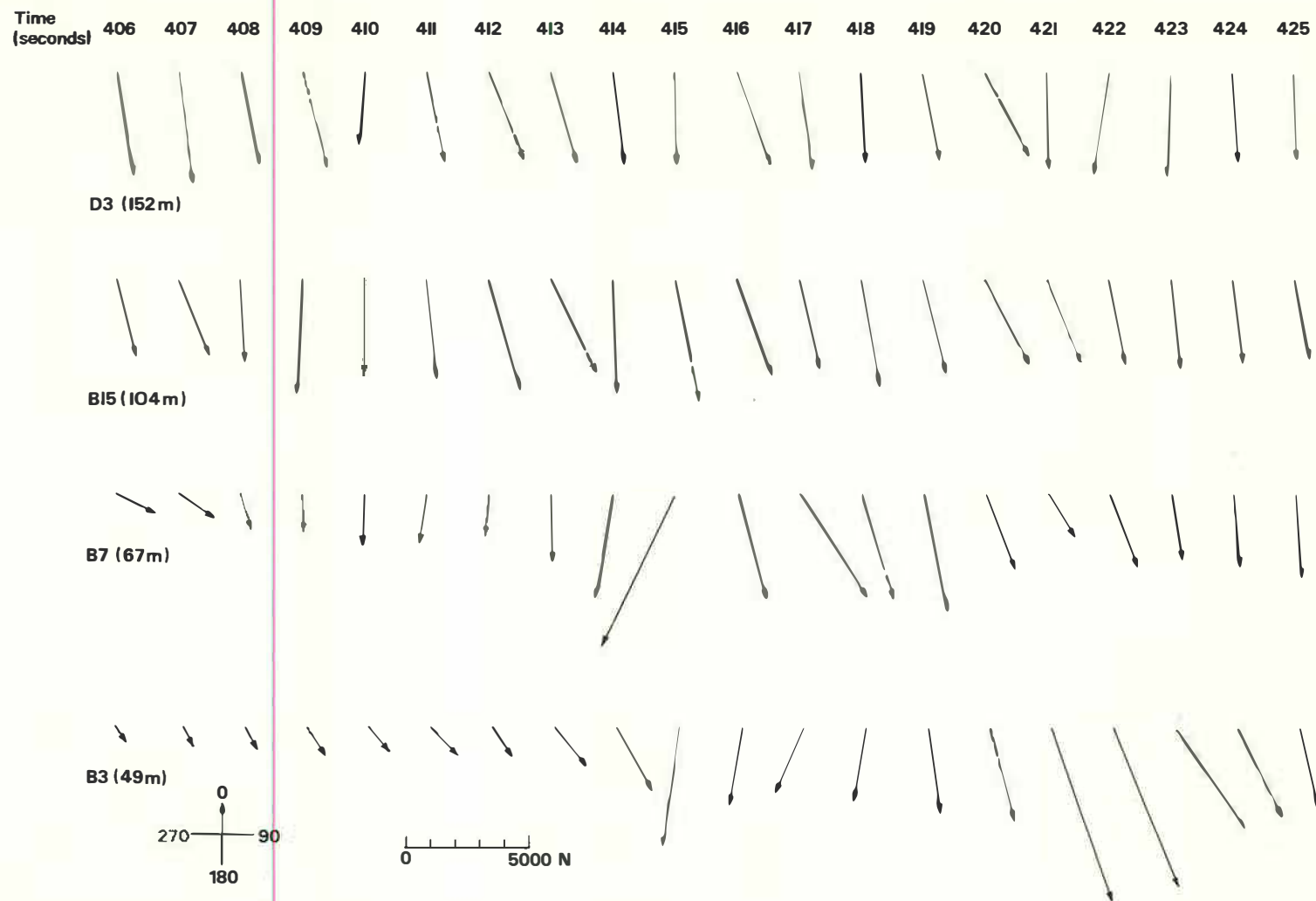


Figure 21 Second-by-second plot of the 1-second load vectors

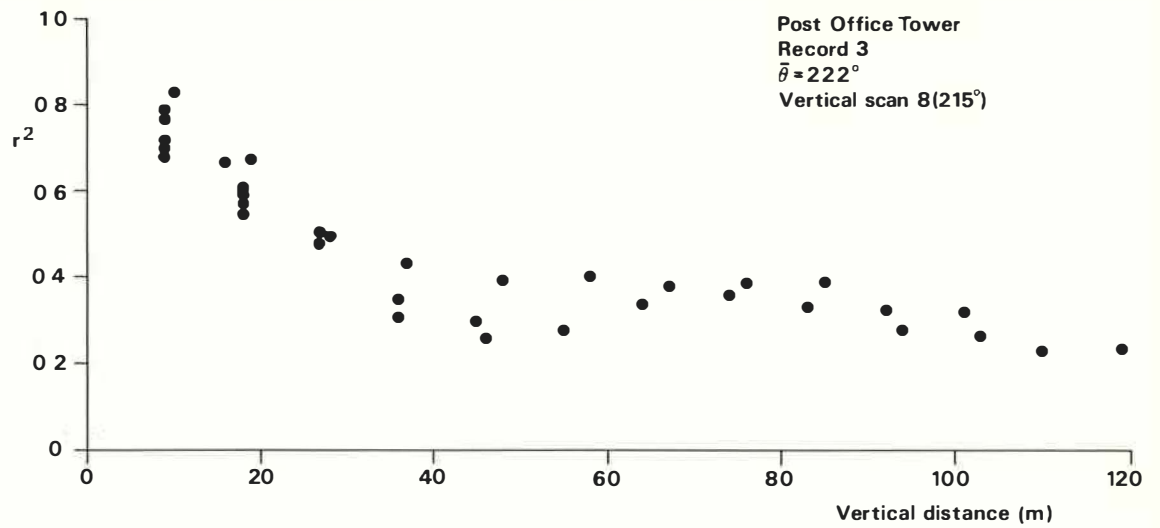


Figure 22 Cross-correlation coefficients, vertical scan 8

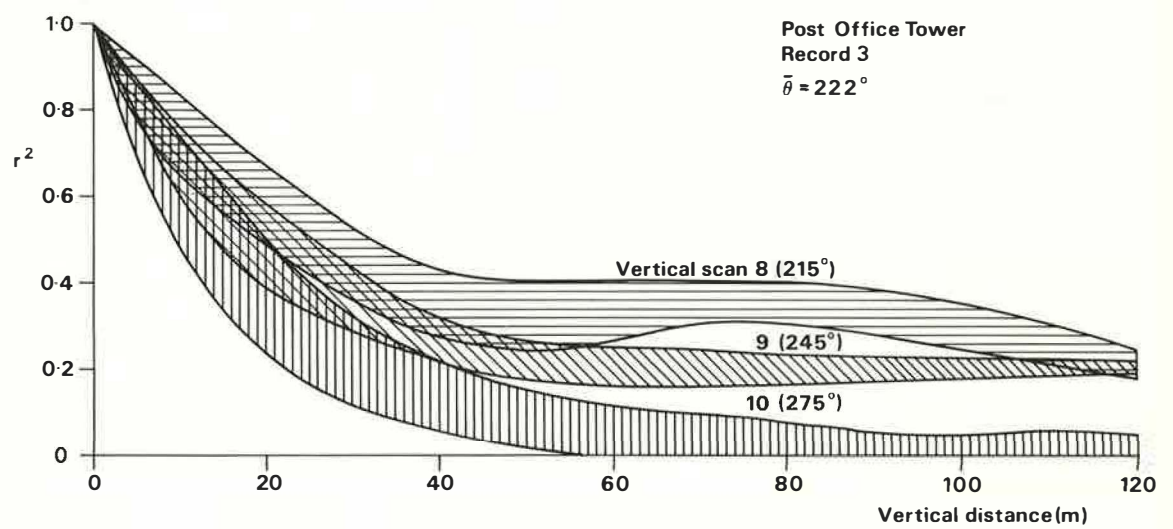


Figure 23 Cross-correlation coefficients, vertical scans 8, 9 and 10

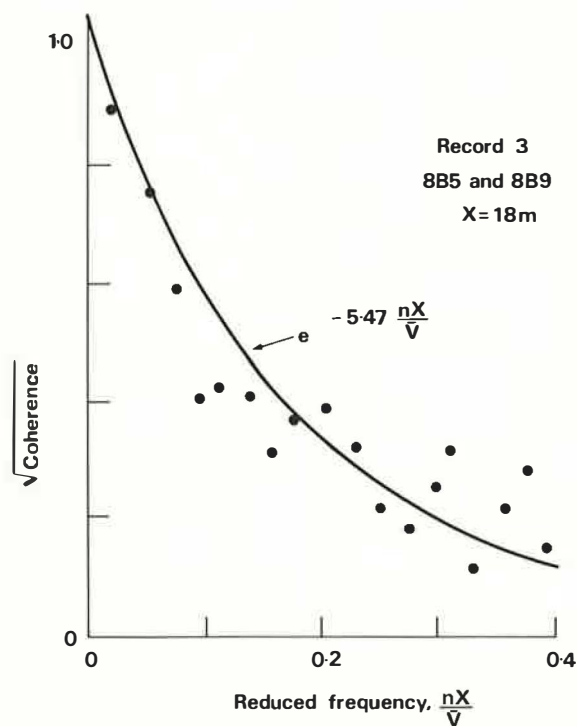


Figure 24 Exponential decay curve for coherence function

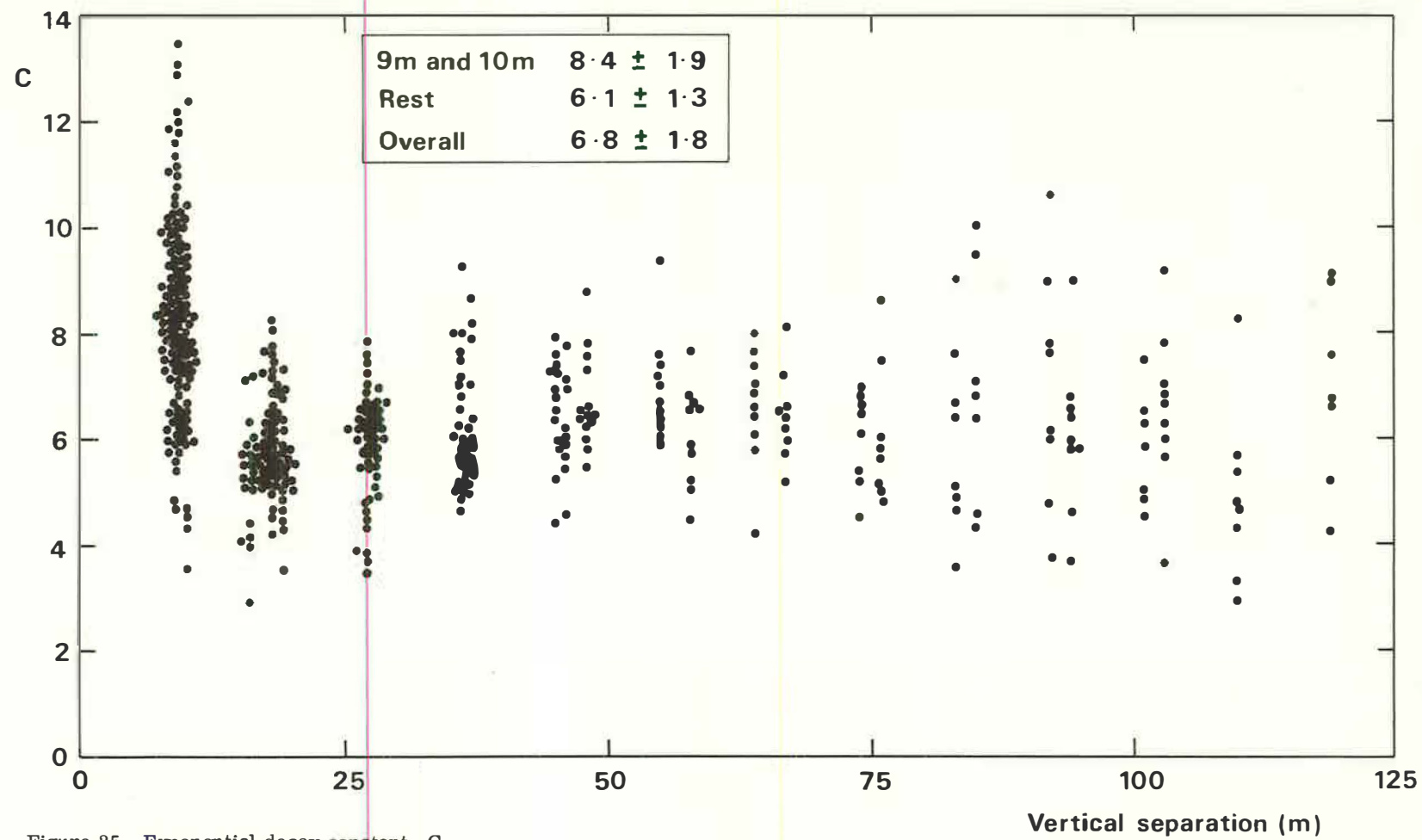


Figure 25 Exponential decay constant, C

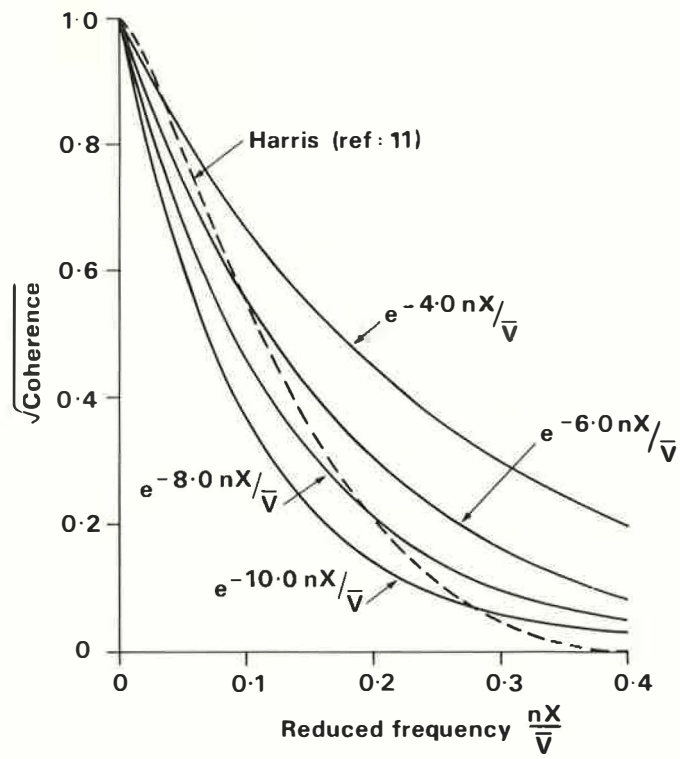


Figure 26 Exponential decay curves for coherence functions

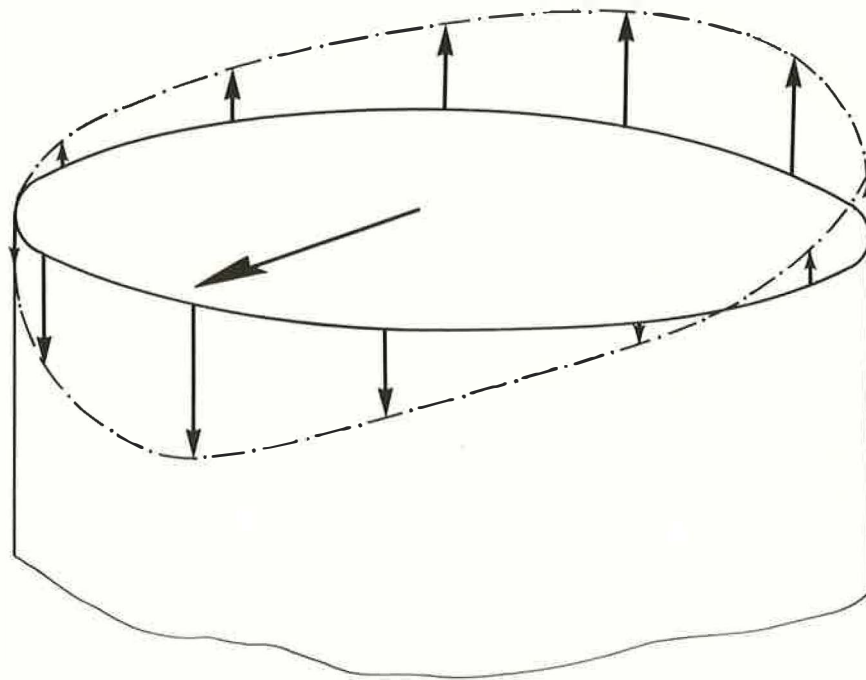


Figure 27 Instantaneous strain distribution

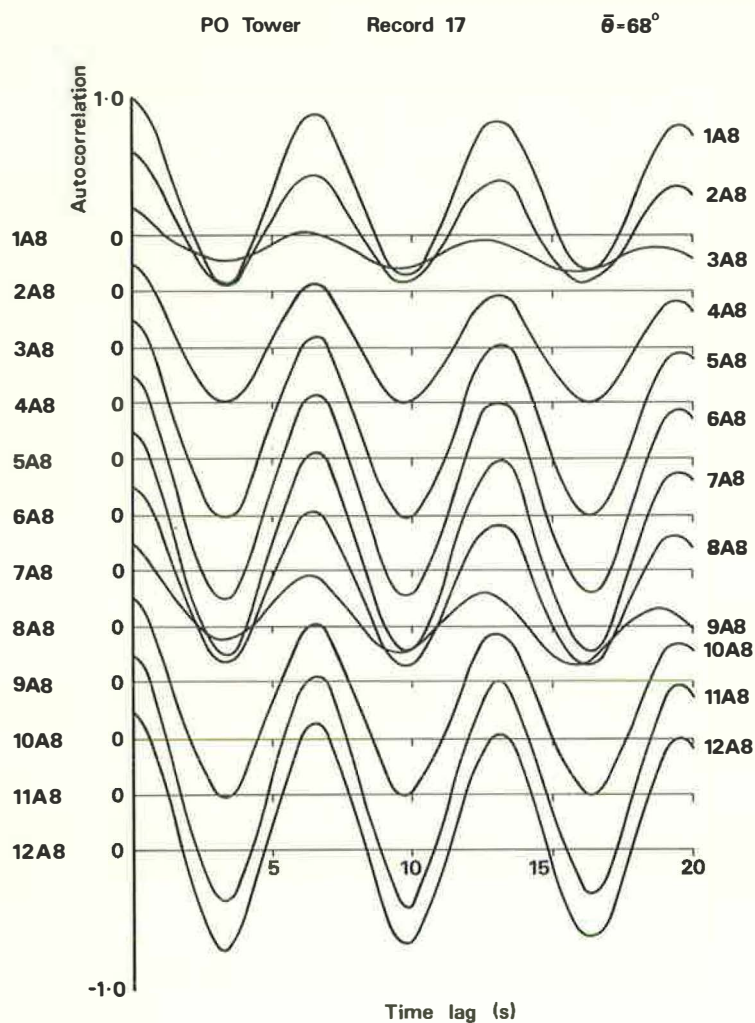


Figure 28 Autocorrelation functions for the strain gauges

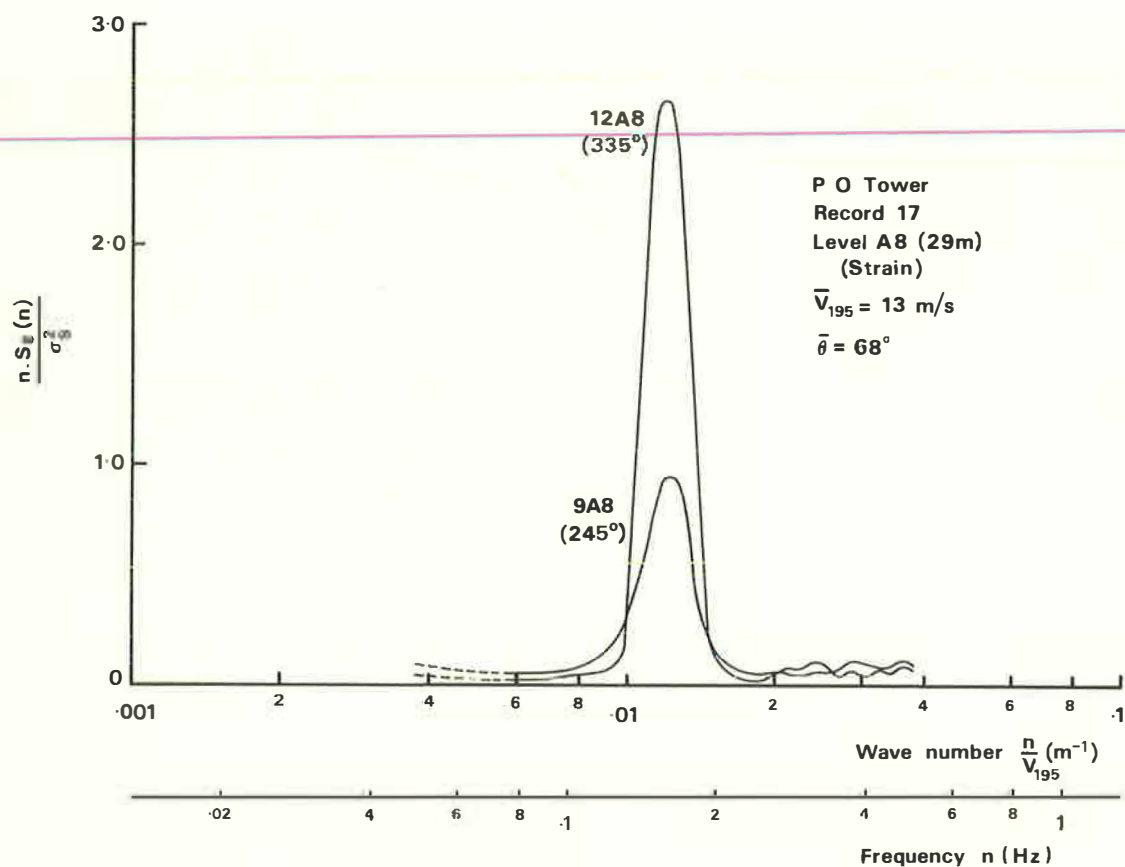


Figure 29 Strain spectra for a side and the leeward gauges

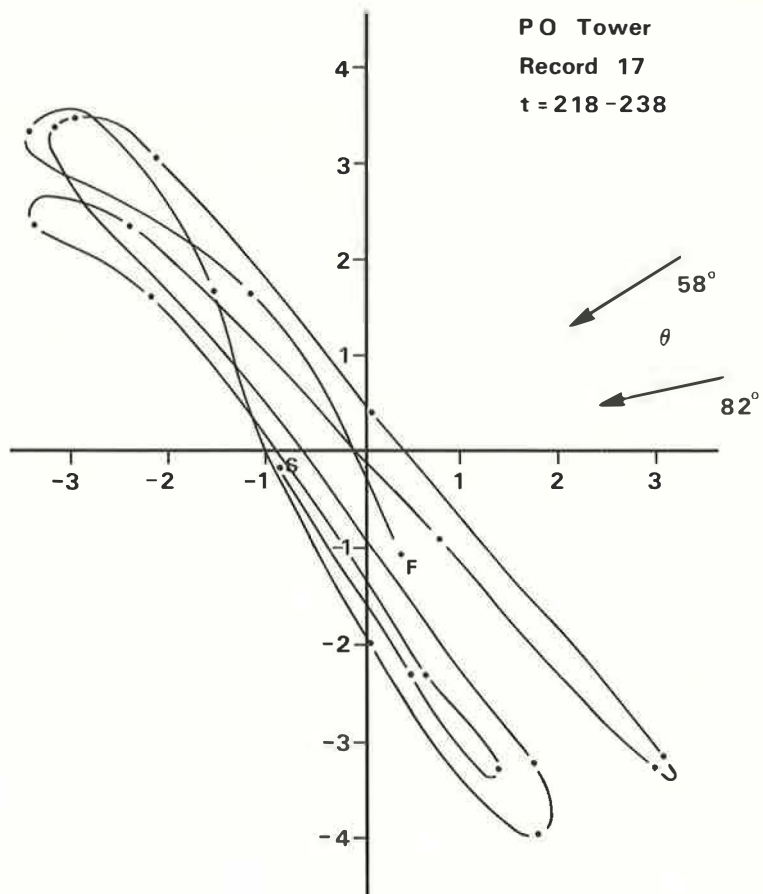


Figure 30

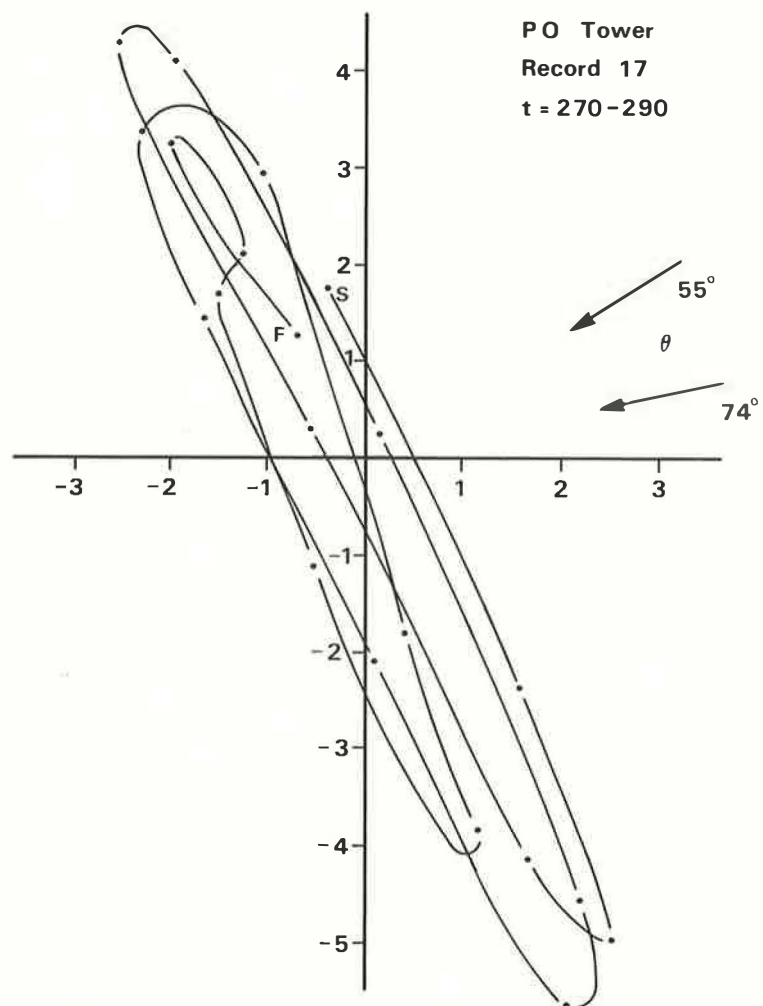


Figure 31

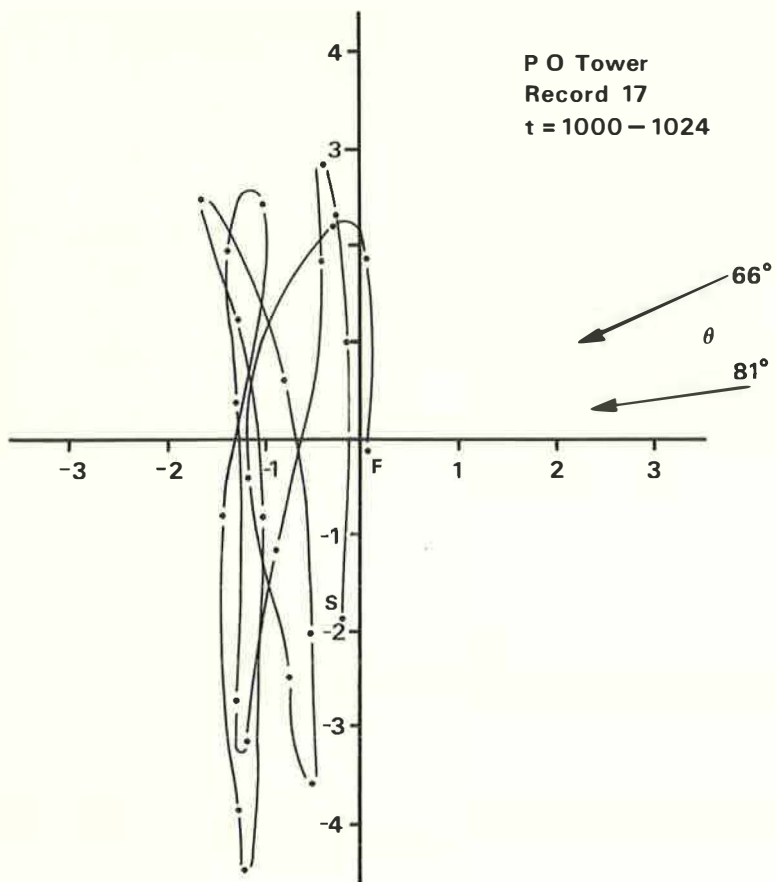


Figure 32

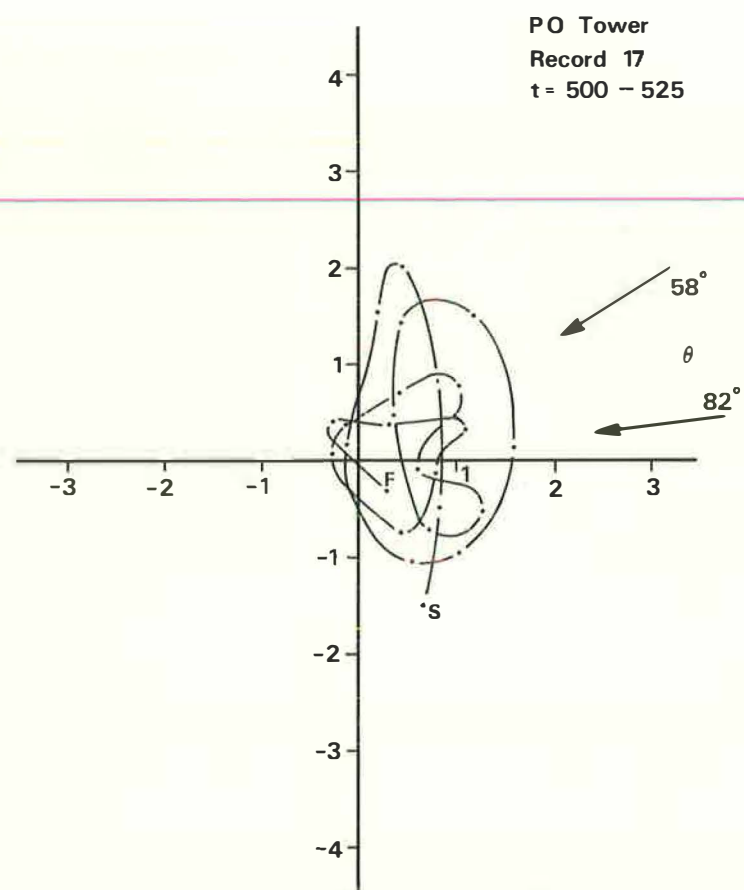


Figure 33

APPENDIX

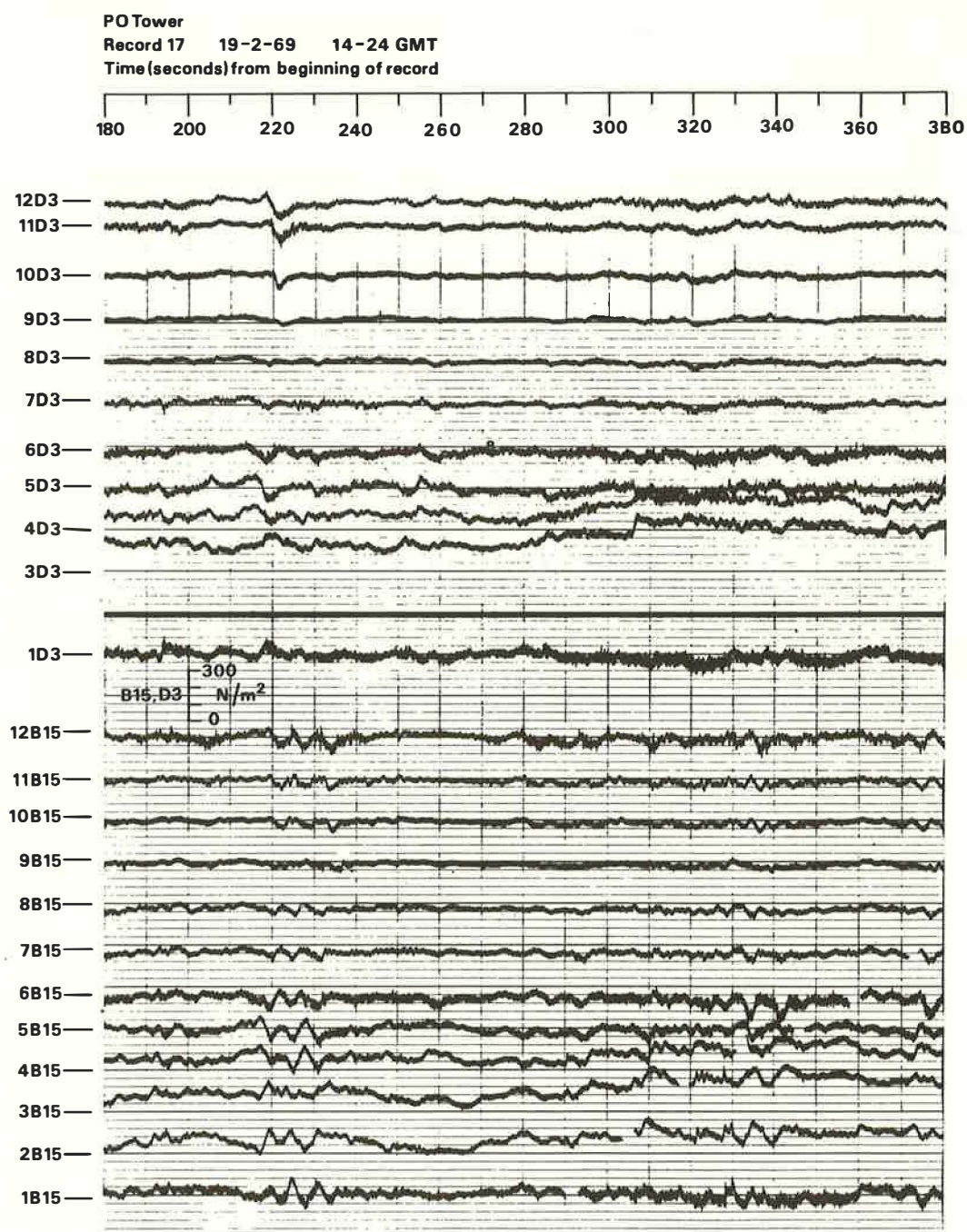


Figure A1

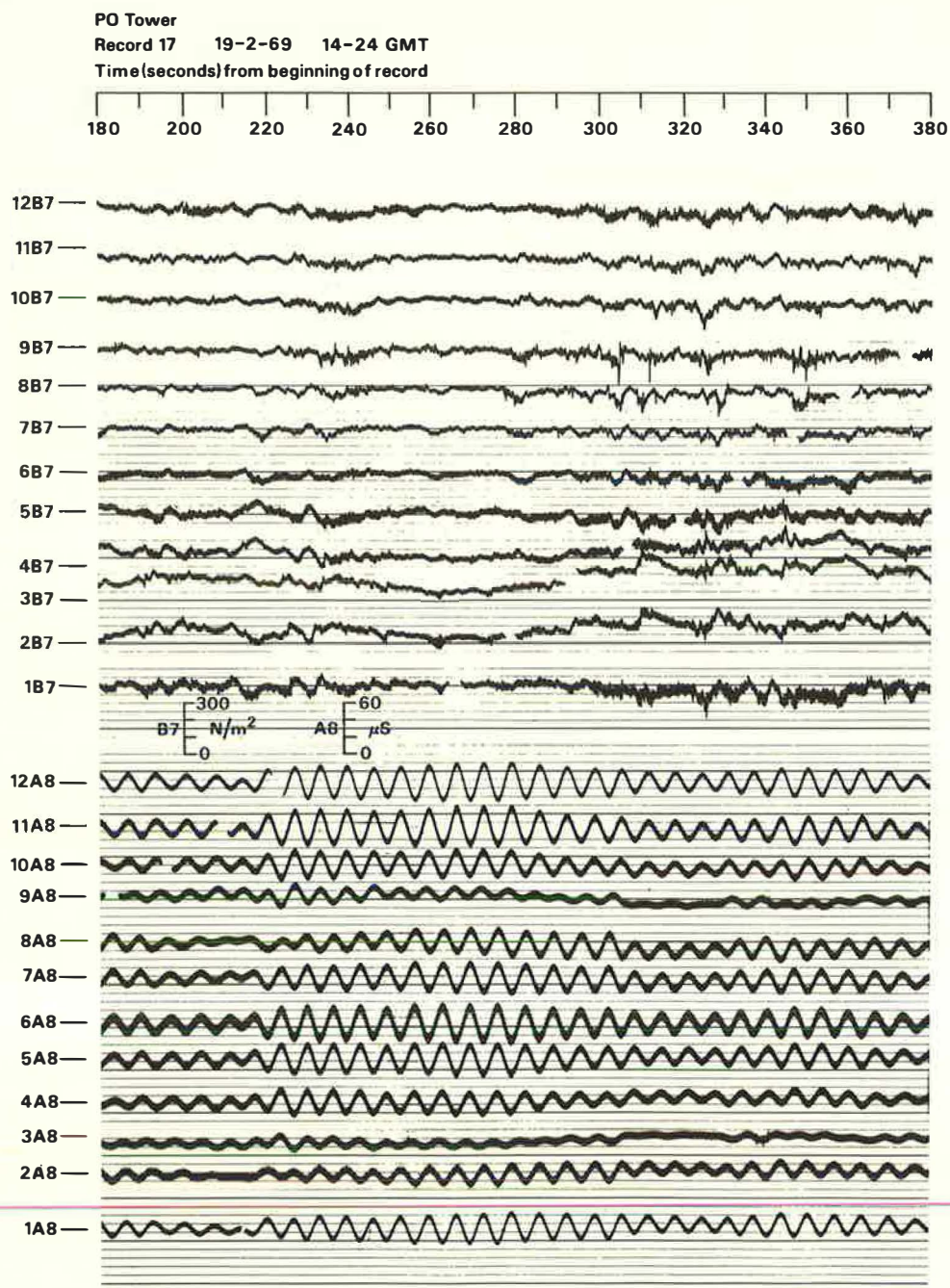


Figure A2

PO Tower
Record 17 19-2-69 14-24 GMT
Data at 1 second intervals from level D3

Time	1D3	3D3	4D3	5D3	6D3	7D3	8D3	9D3	10D3	11D3	12D3	V ₁₉₅	e
275	5	156	52	-26	11	-11	-16	-5	0	-5	-5	21	65
276	5	156	68	-26	16	0	-16	-5	0	-5	-5	20	65
277	5	156	68	-26	0	-5	-5	-5	0	-5	0	18	60
278	21	146	58	-31	-5	0	-5	0	0	0	0	21	64
279	26	172	47	-41	-16	-16	-16	-5	10	5	0	22	67
280	42	167	52	-41	-27	-16	-11	-5	10	0	-5	23	55
281	21	188	79	-36	-16	-5	-16	0	0	-5	-16	22	55
282	0	156	73	-41	0	-16	-16	-5	0	-16	-36	22	58
283	16	172	79	-21	-5	0	-5	0	0	-27	-26	22	60
284	11	198	94	-31	0	0	-5	0	0	-16	-16	23	62
285	26	235	94	-67	-5	-16	-16	-5	0	-5	0	23	67
286	16	229	79	-67	-16	-27	-43	-16	0	-5	-31	25	66
287	5	198	73	-57	-16	-37	-21	-5	-5	-5	-26	25	64
288	-5	198	100	-26	-11	-16	-16	-16	-10	-16	-26	25	66
289	-42	219	94	-47	-16	-27	0	-11	-5	-16	-42	25	65
290	-5	240	105	-41	-5	-16	-5	0	0	-27	-26	25	62
291	0	235	105	-41	0	0	0	0	10	0	-16	25	66
292	16	240	121	-31	-5	-16	-11	11	0	-16	-16	28	63
293	-5	240	142	-21	5	-5	-11	16	15	0	-5	29	68
294	-16	271	152	0	0	-5	0	0	10	-5	-10	27	70
295	-5	250	131	-16	-5	11	5	0	0	0	-5	28	71
296	16	214	147	-16	0	16	5	27	15	-5	5	31	68
297	11	235	168	0	-5	11	21	43	15	0	31	31	65
298	-5	276	194	16	43	11	21	32	20	27	31	30	68
299	-16	250	183	21	16	5	0	27	31	32	0	29	72
300	-42	224	168	31	0	16	0	32	36	22	21	30	69
301	-16	224	178	16	-5	0	0	32	15	0	5	31	67
302	37	219	162	-5	-16	-21	-5	16	20	5	16	29	70
303	0	214	157	5	-5	-5	-16	38	41	5	31	29	68
304	-26	245	162	0	0	0	0	5	15	0	5	30	72
305	-16	240	180	16	-5	11	-5	16	20	-5	5	32	71
306	0	323	220	5	-27	-16	0	16	15	0	0	34	69
307	21	370	252	0	-38	-16	0	0	0	0	16	33	68
308	-58	334	220	-26	-49	-32	-32	0	0	0	10	32	62
309	-58	339	236	5	5	-11	-27	-5	-15	-27	5	29	56
310	-26	297	225	31	5	0	0	16	0	-5	-26	30	55
311	-5	307	204	-41	-60	-16	-5	-5	-5	0	-5	29	58
312	-5	302	189	-47	-27	-16	-16	0	0	0	0	27	61
313	-5	307	199	-21	0	-27	-27	0	10	0	0	30	64
314	-5	302	204	-16	-5	-5	-5	0	0	0	-10	32	61
315	-37	302	199	-16	-5	-5	0	16	0	-5	-5	33	64
316	-5	328	204	-16	-5	-11	-5	0	0	-5	-5	34	64
317	0	307	189	-5	-11	-5	0	0	10	0	0	36	61
318	-16	334	190	-41	-27	-16	-11	11	10	-11	0	36	66
319	-42	344	204	-57	-27	-43	-27	-5	-5	-16	-16	38	68
320	-26	334	204	-41	-49	-48	-48	-16	-26	-43	-21	38	68
321	-47	307	199	-41	-60	-53	-43	-27	-15	-49	-26	38	70
322	-63	323	220	-41	-60	-37	-43	-16	-5	-27	-26	38	68
323	-68	313	215	-26	-49	-27	-27	-16	-10	-5	-26	38	68
324	-26	302	199	-41	-38	-27	-27	-16	-10	-27	-16	37	68
325	-47	292	204	-26	-71	-27	-37	-16	0	-5	-16	31	63
326	-42	302	199	-16	-43	-16	-16	0	0	-16	0	32	69
327	-42	302	204	-16	-38	-5	-16	0	0	-5	-5	37	70
328	-16	302	199	0	-16	-16	-27	0	0	-5	0	34	65
329	0	292	183	-16	-38	-5	-5	0	15	0	16	33	69
330	16	302	183	-16	-43	0	0	16	31	16	21	32	71

Units:

1D3 to 12D3 (Pressure transducers): N/m²

V₁₉₅ (Velocity at height of 195m): knots (1 knot \equiv 0.514 m/s)

θ (Wind direction at 195m): degrees from North

Figure A3

PO Tower

Record 17 19-2-69 14-24 GMT

Data at 1 second intervals from level B15

Time	1B15	2B15	3B15	4B15	5B15	6B15	7B15	8B15	9B15	10B15	11B15	12B15
275	40	71	102	63	0	0	-5	-15	-15	-40	-5	-30
276	55	92	133	63	-5	-5	-5	-15	-5	-25	0	-15
277	60	97	128	63	-20	-25	-15	-26	-10	-25	0	-5
278	75	132	138	52	-31	-15	-25	-26	-5	-25	5	-5
279	90	127	138	31	-41	-25	-20	-41	-15	-10	10	0
280	75	122	148	47	-36	-25	-15	-36	-5	-15	26	-15
281	65	107	123	47	-25	-10	-15	-46	-25	-40	0	-66
282	50	82	117	68	-5	0	0	-26	-15	-55	-16	-56
283	25	56	92	63	0	-5	-5	-5	-25	-55	-26	-86
284	30	66	66	42	-15	-25	-15	-41	-30	-45	-10	-76
285	40	71	82	47	-41	-56	-36	-46	-15	-35	0	-41
286	55	87	92	21	-41	-46	-46	-46	-15	-40	-5	-25
287	65	92	92	42	-41	-41	-41	-46	-25	-45	-16	-41
288	45	87	82	42	-20	-25	-15	-41	-35	-55	-26	-56
289	20	66	107	42	-25	-20	-20	-36	-25	-60	-16	-76
290	25	76	117	68	-15	-20	-15	-41	-35	-55	-16	-66
291	20	31	92	57	-10	-25	-5	-41	-25	-55	-16	-66
292	30	92	97	42	-31	-56	-41	-46	-35	-50	-16	-56
293	25	117	133	31	-61	-66	-41	-56	-30	-45	-5	-15
294	30	112	143	42	-56	-56	-46	-56	-30	-50	-5	-46
295	20	117	163	78	-25	-15	-41	-56	-35	-65	-5	-66
296	0	132	163	104	-10	-5	0	-36	-25	-55	-26	-76
297	5	97	163	94	0	-10	-5	-26	-25	-65	-21	-76
298	25	97	174	99	0	-15	-5	-5	-15	-65	-26	-41
299	40	117	158	104	0	-25	-15	-36	-10	-40	0	-15
300	40	97	143	109	5	-25	-15	-26	-15	-30	10	-15
301	15	76	143	94	0	-41	-10	-36	-15	-40	-5	-30
302	25	76	128	94	0	-31	-5	-26	-10	-15	21	-15
303	45	92	143	94	-5	-25	-15	-36	-15	-15	-5	-25
304	40	82	143	94	-5	-25	-15	-31	-15	-40	-5	-25
305	5	97	163	115	10	-5	-5	-15	-25	-45	-47	-41
306	15	117	204	125	20	-5	0	-10	-15	-40	-41	-41
307	25	122	179	89	-15	-51	-15	-56	-25	-40	-21	-41
308	60	168	214	63	-31	-46	-15	-56	-25	-40	-16	-41
309	55	199	260	63	-66	-36	-36	-41	-15	-45	-47	-96
310	25	178	255	146	-5	-5	-15	-36	-15	-45	-47	-96
311	-5	183	260	167	31	15	20	-10	-15	-40	0	-25
312	40	127	235	146	0	-46	-15	-5	-10	-50	-10	-15
313	10	143	243	167	-25	-25	-41	-31	-10	-30	0	0
314	45	117	199	156	0	-46	-41	-41	-15	-35	0	-5
315	35	112	168	120	15	-25	-15	-41	-40	-25	0	0
316	50	127	194	104	0	-10	-10	-15	-5	-40	5	0
317	65	153	168	120	0	-25	-25	-41	-35	-55	0	0
318	-5	87	158	130	15	5	-5	-46	-15	-55	-31	-46
319	25	92	158	99	-10	-46	-30	-31	-25	-55	-26	-46
320	-5	76	194	151	15	-36	-25	-46	-30	-35	-16	-41
321	0	127	214	172	20	-25	-25	-26	-10	-60	-16	-15
322	-20	117	209	172	-15	-20	-25	-26	-20	-45	0	-15
323	40	143	214	135	-10	-46	-25	-41	-10	-60	-16	-10
324	50	143	204	130	-15	-81	-46	-46	-30	-25	0	0
325	0	92	194	162	15	-10	0	-26	-15	-40	-16	-10
326	-5	107	194	162	10	-41	-15	-10	-15	-45	-16	-10
327	40	122	230	83	-25	-92	-56	-67	-40	-40	-5	-25
328	50	143	194	94	-25	-66	-41	-41	-15	-25	0	0
329	95	194	194	120	0	-31	0	-31	15	-25	0	5
330	45	107	168	146	25	5	15	0	10	-15	16	-36

Units:

1B to 12B15 (Pressure transducers) : N/m²

Figure A4

PO Tower

Record 17 19-2-69 14-24 GMT

Data at 1 second intervals from level B7

Time	1B7	2B7	3B7	4B7	5B7	6B7	7B7	8B7	9B7	10B7	11B7	12B7
275	0	49	65	91	35	20	21	0	0	15	-40	-14
276	31	39	55	91	15	0	0	-15	0	10	-65	-34
277	26	88	85	71	0	0	10	10	0	0	-25	-5
278	0	59	50	76	0	0	-5	-30	0	-5	-55	-10
279	0	59	75	91	0	-25	-16	-41	-15	-10	-74	-39
280	15	29	70	91	5	-40	-16	-51	-29	0	-40	-5
281	21	54	70	81	0	-25	-26	-96	-63	0	-40	-24
282	46	64	75	71	-40	-25	-31	-56	-29	55	0	5
283	57	59	85	76	-30	-30	-16	-41	-10	35	-25	0
284	0	98	90	71	-25	-25	-5	-41	0	30	-40	-5
285	15	88	90	51	-15	0	-5	-15	0	0	-55	-24
286	41	88	80	61	-15	-5	0	-25	-24	5	-45	-5
287	21	78	75	56	-20	5	0	-5	-15	15	-50	-24
288	51	88	70	30	0	5	-21	0	0	5	-40	-24
289	15	69	100	51	-25	0	-26	-5	0	0	-60	-24
290	41	108	95	66	-20	-5	-16	-41	-5	-5	-45	-43
291	15	69	90	66	5	0	-16	-15	0	0	-55	-39
292	5	69	120	76	10	0	0	-5	-24	-5	-74	-48
293	-21	78	135	96	5	40	0	-5	-15	5	-55	-29
294	5	113	155	96	-25	5	-16	-5	-15	-35	-55	-39
295	5	127	150	96	-45	-10	-36	-35	-24	-15	-45	-39
296	51	113	140	66	-40	0	-21	-41	-5	0	-30	-39
297	46	122	155	91	-25	-15	-10	-41	0	15	-25	-24
298	31	113	180	111	-25	-15	-26	-56	-15	25	0	-5
299	31	162	175	91	-20	0	-5	-15	-29	15	-60	-39
300	-10	127	180	91	-15	-10	-5	-15	10	-20	-89	-39
301	-5	108	170	111	-15	-15	0	-35	-39	-40	-114	-92
302	0	103	130	96	-5	-15	-5	5	-15	-30	-94	-72
303	-15	127	160	96	-30	-45	-47	-56	-53	-15	-89	-72
304	-36	103	170	91	-49	-40	-41	-91	-58	-25	-89	-43
305	-26	147	180	116	-40	-10	-10	-96	-15	-25	-70	-63
306	5	88	160	137	25	30	-5	-25	15	-5	-55	-39
307	-15	88	165	131	5	10	0	-5	0	5	-35	-34
308	10	93	150	142	0	-5	-16	-15	-5	-5	-40	-14
309	-41	137	210	157	-35	-35	-47	-56	-44	-5	-45	-39
310	-15	176	255	142	-45	-15	-41	-91	-24	-5	-74	-53
311	10	191	259	131	-35	-10	-26	-56	-63	-15	-70	-43
312	-72	176	240	126	-15	25	0	-25	0	-5	-55	-92
313	-41	186	240	142	-5	-15	-26	-30	-53	-89	-74	-87
314	-5	147	210	111	-25	-30	-57	-41	-44	-25	-94	-43
315	-5	127	195	96	-45	-40	-57	-76	-53	-15	-70	-53
316	-26	127	195	111	-30	-25	-41	-41	-39	-25	-84	-53
317	-15	108	180	121	-15	-10	-5	-25	-29	-15	-114	-63
318	-15	127	160	126	-15	0	0	-15	0	-30	-84	-63
319	10	103	140	96	-40	-5	-16	-25	0	-5	-104	-39
320	0	108	155	111	-25	15	-5	-15	-24	20	-79	-63
321	-5	103	150	96	-35	-35	-41	-46	-24	-5	-45	-63
322	5	108	180	111	-5	-20	-41	-30	-39	-25	-70	-63
323	-41	49	150	116	5	-5	-26	-66	-39	-10	-89	-14
324	-41	103	195	142	-40	-45	-47	-15	-10	-74	-124	-101
325	-154	59	190	197	20	-45	-26	-66	-53	-129	-114	-72
326	-46	113	180	121	-15	-15	5	-41	-112	-74	-109	-121
327	-10	137	195	142	-15	-40	-31	-15	-39	-55	-94	-72
328	46	176	205	91	-94	-65	-88	-56	-39	-35	-65	-63
329	21	157	205	111	-40	-40	-41	-96	-39	0	-55	-43
330	-10	147	185	126	-35	0	-5	-35	-39	-5	-74	-63

Units:

1B7 to 12B7 (Pressure transducers): N/m²

Figure A5

PO Tower
Record 17 19-2-69 14-24 GMT
Data at 1 second intervals from level A8

Time	1A8	2A8	3A8	4A8	5A8	6A8	7A8	8A8	9A8	10A8	11A8	12A8	V ₁₉₅	θ
275	-8	-5	3	15	15	17	11	11	0	-7	-19	-18	21	65
276	-5	-3	0	10	19	16	14	13	2	-5	-17	-14	20	65
277	3	1	0	2	1	0	-3	7	5	1	-3	-3	18	60
278	18	9	-1	-5	-14	-16	-16	-8	7	11	18	14	21	64
279	22	13	0	-5	-14	-13	-19	-11	3	14	21	22	22	67
280	12	3	6	2	-3	-3	-8	-3	0	5	6	8	23	55
281	-3	0	6	8	15	9	3	3	-1	-2	-5	-1	22	55
282	-3	-1	4	12	16	17	8	11	0	-3	-15	-13	22	58
283	0	-3	2	7	11	16	14	12	0	-1	-8	-8	22	60
284	12	4	2	1	-6	-7	-5	0	2	4	4	3	23	62
285	17	8	-1	-1	-8	-12	-16	-7	3	9	10	12	23	67
286	3	6	7	4	0	3	-1	-4	0	1	4	9	25	66
287	-1	0	5	7	10	10	6	5	-1	-1	-10	-4	25	64
288	-5	-3	4	7	8	10	4	5	1	-4	-8	-8	25	66
289	0	-1	4	14	16	17	11	14	0	-4	-9	-12	25	65
290	4	1	3	6	8	10	5	8	3	0	-3	-3	25	62
291	12	8	4	3	1	-3	-8	-1	0	5	7	5	25	66
292	20	15	4	0	-12	-7	-15	-10	0	8	10	12	28	63
293	17	12	10	6	-3	-3	-10	-5	-3	9	9	12	29	68
294	3	5	8	7	5	4	-3	-3	-3	-1	-3	-2	27	70
295	-3	-3	3	10	11	16	8	7	0	-3	-11	-12	28	71
296	1	-3	0	16	17	17	12	11	0	-4	-5	-10	31	68
297	6	5	5	6	1	3	0	0	1	4	-3	-7	31	65
298	14	10	3	0	-1	-5	-10	-7	-1	5	7	7	30	68
299	18	14	8	1	-3	-6	-11	-7	-5	9	8	14	29	72
300	6	6	8	9	0	1	0	-3	-4	0	-5	9	30	69
301	-1	0	5	10	11	12	3	3	-5	-3	-8	-8	31	67
302	-7	-3	3	17	16	16	12	11	0	-1	-15	-12	29	70
303	6	1	0	5	4	7	0	3	3	0	-8	-7	29	68
304	14	10	5	0	-3	-6	-16	-10	0	4	5	5	30	72
305	21	16	9	3	-5	-8	-16	-11	-3	7	9	16	32	71
306	15	13	11	6	0	-2	-12	-11	-7	0	4	10	34	69
307	3	5	8	10	10	5	-1	-3	-8	-4	-8	-4	33	68
308	0	1	9	17	15	12	2	0	-8	-7	-15	-12	32	62
309	3	4	8	11	8	8	0	0	-8	-7	-11	-6	29	56
310	14	9	10	3	1	-1	-8	-7	-8	0	-2	3	30	55
311	17	15	8	4	-4	-7	-16	-16	-7	4	6	9	29	58
312	13	13	8	5	-1	-2	-13	-13	-8	2	6	11	27	61
313	9	10	10	9	5	2	-5	-8	-8	0	-3	0	30	64
314	0	2	9	12	10	9	0	-1	-8	-7	-9	-7	32	61
315	0	2	8	14	15	12	2	1	-7	-4	-11	-8	33	64
316	10	8	8	7	4	2	-5	-8	-5	-1	-3	-1	34	64
317	16	13	8	5	-3	-4	-14	-11	-3	4	3	6	36	61
318	16	12	10	5	-1	-4	-14	-12	-5	4	8	8	36	66
319	11	10	10	7	1	0	-8	-8	-6	0	3	4	38	68
320	4	4	9	13	9	7	-1	-4	-8	-4	-9	-4	38	68
321	1	2	9	17	16	11	3	0	-8	-7	-15	-8	38	70
322	9	7	11	14	10	5	0	-3	-8	-4	-9	-4	38	68
323	12	10	9	7	1	-2	-8	-10	-8	-2	-3	2	38	68
324	14	14	10	6	0	-5	-14	-11	-8	2	3	7	37	68
325	13	10	8	6	0	-3	-12	-10	-8	3	2	7	31	63
326	7	8	12	9	5	4	-6	-7	-8	-1	-3	0	32	69
327	2	3	9	12	11	9	0	0	-8	-4	-11	-8	37	70
328	0	1	8	14	14	9	3	-1	-8	-7	-11	-8	34	65
329	10	8	6	6	5	1	-8	-7	-5	-1	-5	0	33	69
330	12	11	6	4	-5	-8	-15	-10	-3	0	2	5	32	71

Units:

1A8 to 12A8 (Strain gauges): Dimensionless(Micro-strain)

V₁₉₅(Velocity at height of 195m): knots(1knot≡0.514 m/s)

θ(Wind direction at 195m): degrees from North

Figure A6

Current papers — recent issues

CP28/71	The structure of building control—an international comparison.	EVELYN CIBULA
CP29/71	Strain measurements at the GPO Tower, London.	K J EATON and J R MAYNE
CP30/71	Some field techniques for improving site investigation and engineering design.	W H WARD
CP31/71	The effects of ventilation and building design factors on the risk of condensation and mould growth in dwellings.	A G LOUDON
CP32/71	Measuring movements of engineering structures.	A D M PENMAN and J A CHARLES
CP33/71	Experiments on the rain penetration of brickwork: the effect of mortar type.	J W SKEEN
CP34/71	Dimensional disciplines and the output of bricklayers: a case study.	W S FORBES
CP35/71	Wind damage to buildings in the United Kingdom 1962-1969.	J B MENZIES
CP36/71	Tests of a full-scale rigid-jointed multi-storey steel frame in high-yield steel (BS 4360, Grade 50)	E H ROBERTS and R F SMITH
CP37/71	Wind pressures on the Post Office Tower, London.	C W NEWBERRY, K J EATON and J R MAYNE
CP38/71	Investigation of maintenance and energy costs for services in office buildings.	N O MILBANK, J P DOWDALL and A SLATER
CP39/71	Cost benefits from variety reduction in standard steel windows.	D W PEDDER-SMITH
CP40/71	Building materials management: unit loads and fork-lift trucks.	E A AKAM
CP1/72	Instrumentation for embankment dams subjected to rapid drawdown.	A D M PENMAN
CP2/72	On the stiffnesses and strengths of infilled frames.	R J MAINSTONE
CP3/72	The influence of a bounding frame on the racking stiffnesses and strengths of brick walls.	R J MAINSTONE and G A WEEKS
CP4/72	An investigation of the use of water outlets in multi-storey flats.	C J D WEBSTER
CP5/72	Survey of meteorological information for architecture and building.	R E LACY
CP6/72	Pore pressures and displacements beneath embankments on soft natural clay deposits.	J B BURLAND
CP7/72	Factors influencing the choice of tolerances.	T J GRIFFITHS
CP8/72	Observation of retaining wall movements associated with a large excavation.	K W COLE and J B BURLAND
CP9/72	Slab design: past, present and future.	R H WOOD
CP10/72	Office building: needs of small firms.	FLORA W BLACK
CP11/72	A simple and precise borehole extensometer.	J B BURLAND, J F A MOORE and P D K SMITH
CP12/72	Demolition	E A AKAM
CP13/72	'Social' housing in Europe.	EVELYN CIBULA
CP14/72	Aggregates from waste materials.	W GUTT
CP15/72	Internal cracking in reinforced concrete.	J M ILLSTON and R F STEVENS
CP16/72	Model studies of deep in-situ loading tests in clay.	A MARSLAND
CP17/72	Glass fibre reinforced cement.	B R STEELE
CP18/72	Effect of the position of the core on the behaviour of two rockfill dams.	A D M PENMAN and J A CHARLES
CP19/72	Constructional deformations in a rockfill dam.	A D M PENMAN and J A CHARLES
CP20/72	Tests on assemblies of large precast concrete panels.	G S T ARMER and S KUMAR
CP21/72	Housing at Llanedeyrn, built with L-shaped precast panels.	K J SEYMOUR-WALKER
CP22/72	Causes and control of dimensional variations in light steel frames.	R M MILNER
CP23/72	The Finchampstead project.	W S FORBES and ROSEMARY STJERNSTEDT

Current papers — recent issues

CP1/73	Large in-situ tests to measure the properties of stiff fissured clays.	A MARSLAND
CP2/73	Accuracy and its structural implications for loadbearing brick constructions.	R M MILNER and R P THOROGOOD
CP3/73	Deflections of reinforced concrete beams.	R F STEVENS
CP4/73	Refuse collection from houses and flats by pipeline.	R G COURTNEY and D E SEXTON
CP5/73	In-situ plate tests in lined and unlined boreholes in highly fissured London Clay.	A MARSLAND
CP6/73	Designing offices against traffic noise—environmental standards, design principles, engineering requirements.	A F E WISE
CP7/73	The economics of lightweight aggregate structural concrete.	E R SKOYLES
CP8/73	Notes on the CEB Draft Practice Manual on lightweight concrete.	A SHORT
CP9/73	Research for better sanitary services.	A F E WISE
CP10/73	Width variations of cladding joints.	M R M HERBERT and J L CRONSHAW
CP11/73	The hazard of internal blast in buildings.	R J MAINSTONE
CP12/73	Studies of refuse compaction and incineration in multi-storey flats.	D E SEXTON
CP13/73	The use of ground strain measurements in civil engineering.	W H WARD and J B BURLAND
CP14/73	Long-term cracking in reinforced concrete beams.	J M ILLSTON and R F STEVENS
CP15/73	Statistical analysis from a sound level meter.	W E SCHOLES and A C SALVIDGE
CP16/73	Long term unrestrained expansion of test bricks.	R G SMITH
CP17/73	The BRE ultra-violet sensor.	P B HARRIS
CP18/73	Working drawings in use.	C D DALTRY and D T CRAWSHAW
CP19/73	The 1972 CIB Master Lists: their use in the preparation of technical literature.	H J ELDRIDGE
CP20/73	Three-dimensional anisotropic consolidation of clay	P I LEWIN
CP21/73	Appraisal of the weathering behaviour of plastics.	E CAPRON, J R CROWDER and R G SMITH
CP22/73	Research in support of the 1971 revision of BS 368: precast concrete flags.	D F CORNELIUS, J J KOLLEK and D C TEYCHENNÉ
CP23/73	The effect of rate of loading on plain concrete.	P R SPARKS and J B MENZIES
CP24/73	Laboratory and in-situ measurements of the deformation moduli of London Clay.	A MARSLAND
CP25/73	Rigid-jointed multi-storey steel frame design: a state-of-the-art report.	R H WOOD
CP26/73	Contributions to the BGS symposium on field instrumentation.	J B BURLAND et al
CP27/73	A case study of a design commission: problems highlighted; initiatives proposed.	J J N O'REILLY
CP28/73	Strains and displacements around friction piles.	R W COOKE and G PRICE
CP29/73	Wind loading on tall buildings — further results from Royex House.	CW NEWBERRY, KJ EATON and JR MAYNE
CP30/73	Wind pressure and strain measurements at the Post Office Tower.	CW NEWBERRY, KJ EATON and JR MAYNE